(MMP)-3, MMP-9, and MMP-13, in streptococcal cell wall-induced arthritis (43). IL-17R-deficient (IL-17R$^{-/-}$) mice that were locally injected five times with streptococcal cell wall fragments into the knee joints showed a significant reduction of joint thickness and cartilage damage that was accompanied by reduced synovial expression of IL-1, IL-6, and the MMPs 3, 9, and 13 compared with arthritic wild-type mice. Therefore, these results indicate the critical role of IL-17R signaling during progression from an acute, macrophage-driven joint inflammation to a chronic, cartilage-destructive, T cell-mediated synovitis. There are four additional receptor-like molecules that share homology to IL-17R, i.e., IL-17Rh1 (also named IL-17RB or IL-17BR), IL-17RL (also named IL-17RC), IL-17RD, and IL-17RE. IL-17Rh1 was shown to bind to IL-17B, but with higher affinity to IL-17E (11, 12).

Although IL-17A transgenic mice have been reported to be embryonic lethal (39), we established BM-overexpressing mice that constitutively expressed IL-17A. The adequate control of the expression level was critically important. In our experiment, the serum concentration of IL-17A was elevated to ~600 pg/ml in IL-17A BM chimeric mice. This serum concentration of IL-17A was similar to those in patients with inflammatory diseases such as RA, inflammatory bowel diseases, familial Mediterranean fever, and the acute stage of Kawasaki disease (3, 44–46). Therefore, our BM chimeric mice approach may be useful to elucidate the physiological role of inflammatory cytokines that show lethal phenotypes in the conventional gene-transgenic technique.

In conclusion, we found that IL-17 family genes were up-regulated in association with their receptors in CIA. Each of the IL-17 family members clearly exacerbated the progression of CIA with the method of retrovirus-mediated BM chimeric mice. IL-17B and IL-17C have the capacity to exacerbate inflammatory arthritis in association with increased TNF-α and IL-6 productions from macrophages. Moreover, neutralization of IL-17B significantly suppressed the progression of arthritis and bone destruction in CIA mice. Therefore, our results suggest that not only IL-17A, but also the IL-17 family members IL-17B, IL-17C, and IL-17F play an important role in the pathogenesis of inflammatory arthritis and should be a new therapeutic target of arthritis.

Acknowledgments

We are grateful to Yayoi Tsukahara and Kayako Watada for their excellent technical assistance.

Disclosures

The authors have no financial conflict of interest.

References

1. Yao, Z., W. C. Fanslow, M. F. Seldin, A. M. Rousseau, S. L. Painter, M. R. Comeau, J. I. Cohen, and M. K. Spriggs. 1995. Herpesvirus Saimiri encodes a new cytokine: IL-17, which binds to a novel cytokine receptor. *Immunity* 3: 811–821.
2. Yao, Z., S. L. Painter, W. C. Fanslow, D. Ulrich, B. M. Macduff, M. K. Spriggs, and R. J. Armitage. 1995. Human IL-17: a novel cytokine derived from T cells. *J. Immunol.* 155: 5483–5486.
3. Ziolkowska, M., A. Koc, G. Luszczykiewicz, K. Ksiezopolska-Pietrzak, E. Klimczak, H. Chwalinska-Sadowska, and W. Maslinski. 2000. High levels of IL-17 in rheumatoid arthritis patients: IL-15 triggers in vitro IL-17 production via cyclosporin A-sensitive mechanism. *J. Immunol.* 164: 2832–2838.
4. Jovanovic, D. V., J. A. Di Battista, J. Martel-Pelletier, F. C. Jolicoeur, Y. He, M. Zhang, F. Mineau, and J. P. Pelletier. 1998. IL-17 stimulates the production and expression of proinflammatory cytokines IL-β and TNF-α, by human macrophages. *J. Immunol.* 160: 3513–3521.
5. Chabaud, M., F. Fossiez, J. L. Taupin, and P. Miossec. 1998. Enhancing effect of IL-17 on IL-1-induced IL-6 and leukemia inhibitory factor production by rheumatoid arthritis synoviocytes and its regulation by Th2 cytokines. *J. Immunol.* 161: 409–414.
6. Katz, Y., O. Nadiv, and Y. Beer. 2001. Interleukin-17 enhances tumor necrosis factor α-induced synthesis of interleukins 1, 6, and 8 in skin and synovial fibroblasts: a possible role as a "fine-tuning cytokine" in inflammation processes. *Arthritis Rheum.* 44: 2176–2184.
7. Lubberts, E., L. A. Joosten, B. Oppers, L. van den Bersselaar, C. J. Coenen-de Roo, J. K. Kolls, P. Schwarzenberger, F. A. van de Loo, and W. B. van den Berg. 2001. IL-1-independent role of IL-17 in synovial inflammation and joint destruction during collagen-induced arthritis. *J. Immunol.* 167: 1004–1013.
8. Lubberts, E., M. I. Koenders, B. Oppers-Walgreen, L. van den Bersselaar, C. J. Coenen-de Roo, L. A. Joosten, and W. B. van den Berg. 2004. Treatment with a neutralizing anti-murine interleukin-17 antibody after the onset of collagen-induced arthritis reduces joint inflammation, cartilage destruction, and bone erosion. *Arthritis Rheum.* 50: 650–659.
9. Nakae, S., S. Saijo, R. Horai, K. Sudo, S. Mori, and Y. Iwakura. 2003. IL-17 production from activated T cells is required for the spontaneous development of destructive arthritis in mice deficient in IL-1 receptor antagonist. *Proc. Natl. Acad. Sci. USA* 100: 5986–5990.
10. Koenders, M. I., E. Lubberts, F. A. van de Loo, B. Oppers-Walgreen, L. van den Bersselaar, M. M. Helsen, J. K. Kolls, F. E. Di Padova, L. A. Joosten, and W. B. van den Berg. 2006. Interleukin-17 acts independently of TNF-α under arthritic conditions. *J. Immunol.* 176: 6262–6269.
11. Moseley, T. A., D. R. Haudenschild, L. Rose, and A. H. Reddi. 2003. Interleukin-17 family and IL-17 receptors. *Cytokine Growth Factor Rev.* 14: 155–174.
12. Kolls, J. K., and A. Linden. 2004. Interleukin-17 family members and inflammation. *Immunity* 21: 467–476.
13. Starnes, T., M. J. Robertson, G. Sledge, S. Kelich, H. Nakshatri, H. E. Broxmeyer, and R. Hromas. 2001. Cutting edge: IL-17F, a novel cytokine selectively expressed in activated T cells and monocytes, regulates angiogenesis and endothelial cell cytokine production. *J. Immunol.* 167: 4137–4140.
14. Aggarwal, S., N. Ghilardi, M. H. Xie, F. J. de Sauvage, and A. L. Gurney. 2003. Interleukin-23 promotes a distinct CD4 T cell activation state characterized by the production of interleukin-17. *J. Biol. Chem.* 278: 1910–1914.
15. Happel, K. I., P. J. Dubin, M. Zheng, N. Ghilardi, C. Lockhart, L. J. Quinton, A. R. Odden, J. E. Shellito, G. J. Bagby, S. Nelson, and J. K. Kolls. 2005. Divergent roles of IL-23 and IL-12 in host defense against *Klebsiella pneumoniae*. *J. Exp. Med.* 202: 761–769.
16. Shi, Y., S. J. Ullrich, J. Zhang, K. Connolly, K. J. Grzegorzewski, M. C. Barber, W. Wang, K. Wathen, V. Hodge, C. L. Fisher, et al. 2000. A novel cytokine receptor-ligand pair: identification, molecular characterization, and in vivo immunomodulatory activity. *J. Biol. Chem.* 275: 19167–19176.
17. Li, H., J. Chen, A. Huang, J. Stinson, S. Heldens, J. Foster, P. Dowd, A. L. Gurney, and W. I. Wood. 2000. Cloning and characterization of IL-17B and IL-17C, two new members of the IL-17 cytokine family. *Proc. Natl. Acad. Sci. USA* 97: 773–778.
18. Hurst, S. D., T. Muchamuel, D. M. Gorman, J. M. Gilbert, T. Clifford, S. Kwan, S. Menon, B. Seymour, C. Jackson, T. T. Kung, et al. 2002. New IL-17 family members promote Th1 or Th2 responses in the lung: in vivo function of the novel cytokine IL-25. *J. Immunol.* 169: 443–453.
19. Chabaud, M., J. M. Durand, N. Buchs, F. Fossiez, G. Page, L. Frappart, and P. Miossec. 1999. Human interleukin-17: a T cell-derived proinflammatory cytokine produced by the rheumatoid synovium. *Arthritis Rheum.* 42: 963–970.
20. Hymowitz, S. G., E. H. Filvaroff, J. P. Yin, J. Lee, L. Cai, P. Risser, M. Maruoka, W. Mao, J. Foster, R. F. Kelley, et al. 2001. IL-17s adopt a cystine knot fold: structure and activity of a novel cytokine, IL-17F, and implications for receptor binding. *EMBO J.* 20: 5332–5341.
21. Hwang, S. Y., and H. Y. Kim. 2005. Expression of IL-17 homologs and their receptors in the synovial cells of rheumatoid arthritis patients. *Mol. Cell* 19: 180–184.
22. Nasu, K., H. Kohsaka, Y. Nonomura, Y. Terada, H. Ito, K. Hirokawa, and N. Miyasaka. 2000. Adenoviral transfer of cyclin-dependent kinase inhibitor genes suppresses collagen-induced arthritis in mice. *J. Immunol.* 165: 7246–7252.
23. Trentham, D. E., A. S. Townes, and A. H. Kang. 1977. Autoimmunity to type II collagen an experimental model of arthritis. *J. Exp. Med.* 146: 857–868.
24. Stuart, J. M., A. S. Townes, and A. H. Kang. 1982. Nature and specificity of the immune response to collagen in type II collagen-induced arthritis in mice. *J. Clin. Invest.* 69: 673–683.
25. Gerlag, D. M., L. Ransone, P. P. Tak, Z. Han, M. Palanki, M. S. Barbosa, D. Boyle, A. M. Manning, and G. S. Firestein. 2000. The effect of a T cell-specific NF-κB inhibitor on in vitro cytokine production and collagen-induced arthritis. *J. Immunol.* 165: 1652–1658.
26. Nanki, T., Y. Urasaki, T. Imai, M. Nishimura, K. Muramoto, T. Kubota, and N. Miyasaka. 2004. Inhibition of fractalkine ameliorates murine collagen-induced arthritis. *J. Immunol.* 173: 7010–7016.
27. Unkeless, J. C., S. Gordon, and E. Reich. 1974. Secretion of plasminogen activator by stimulated macrophages. *J. Exp. Med.* 139: 834–850.
28. Cheng, E. H., M. C. Wei, S. Weiler, R. A. Flavell, T. W. Mak, T. Lindsten, and S. J. Korsmeyer. 2001. BCL-2. Bcl-x$_L$ sequester BH3 domain-only molecules preventing BAX- and BAK-mediated mitochondrial apoptosis. *Mol. Cell* 8: 705–711.
29. Morita, S., T. Kojima, and T. Kitamura. 2000. Plat-E: an efficient and stable system for transient packaging of retroviruses. *Gene Ther.* 7: 1063–1066.
30. Fujio, K., Y. Misaki, K. Setoguchi, S. Morita, K. Kawahata, I. Kato, T. Nosaka, K. Yamamoto, and T. Kitamura. 2000. Functional reconstitution of class II MHC-restricted T cell immunity mediated by retroviral transfer of the $\alpha\beta$ TCR complex. *J. Immunol.* 165: 528–532.
31. Fujio, K., A. Okamoto, H. Tahara, M. Abe, Y. Jiang, T. Kitamura, S. Hirose, and K. Yamamoto. 2004. Nucleosome-specific regulatory T cells engineered by triple gene transfer suppress a systemic autoimmune disease. *J. Immunol.* 173: 2118–2125.

32. McGaha, T. L., B. Sorrentino, and J. V. Ravetch. 2005. Restoration of tolerance in lupus by targeted inhibitory receptor expression. *Science* 307: 590–593.
33. Livak, K. J., and T. D. Schmittgen. 2001. Analysis of relative gene expression data using real-time quantitative PCR and the $2(-\delta\delta C_T)$ method. *Methods* 25: 402–408.
34. Ferreira, I. D., V. E. Rosario, and P. V. Cravo. 2006. Real-time quantitative PCR with SYBR Green I detection for estimating copy numbers of nine drug resistance candidate genes in *Plasmodium falciparum*. *Malar J.* 5: 1.
35. Corthay, A., A. Johansson, M. Vestberg, and R. Holmdahl. 1999. Collagen-induced arthritis development requires $\alpha\beta$ T cells but not $\gamma\delta$ T cells: studies with T cell-deficient (TCR mutant) mice. *Int. Immunol.* 11: 1065–1073.
36. Glansbeek, H. L., P. M. van der Kraan, F. P. Lafeber, E. L. Vitters, and W. B. van den Berg. 1997. Species-specific expression of type II TGF-β receptor isoforms by articular chondrocytes: effect of proteoglycan depletion and aging. *Cytokine* 9: 347–351.
37. Taniguchi, K., H. Kohsaka, N. Inoue, Y. Terada, H. Ito, K. Hirokawa, and N. Miyasaka. 1999. Induction of the p16INK4a senescence gene as a new therapeutic strategy for the treatment of rheumatoid arthritis. *Nat. Med.* 5: 760–767.
38. Honorati, M. C., R. Meliconi, L. Pulsatelli, S. Cane, L. Frizziero, and A. Facchini. 2001. High in vivo expression of interleukin-17 receptor in synovial endothelial cells and chondrocytes from arthritis patients. *Rheumatology* 40: 522–527.
39. Schwarzenberger, P., V. La Russa, A. Miller, P. Ye, W. Huang, A. Zieske, S. Nelson, G. J. Bagby, D. Stoltz, R. L. Mynatt, et al. 1998. IL-17 stimulates granulopoiesis in mice: use of an alternate, novel gene therapy-derived method for in vivo evaluation of cytokines. *J. Immunol.* 161: 6383–6389.
40. Lubberts, E., L. van den Bersselaar, B. Oppers-Walgreen, P. Schwarzenberger, C. J. Coenen-de Roo, J. K. Kolls, L. A. Joosten, and W. B. van den Berg. 2003. IL-17 promotes bone erosion in murine collagen-induced arthritis through loss of the receptor activator of NF-κB ligand/osteoprotegerin balance. *J. Immunol.* 170: 2655–2662.
41. Mangan, P. R., L. E. Harrington, D. B. O'Quinn, W. S. Helms, D. C. Bullard, C. O. Elson, R. D. Hatton, S. M. Wahl, T. R. Schoeb, and C. T. Weaver. 2006. Transforming growth factor-β induces development of the T_H17 lineage. *Nature* 441: 231–234.
42. Hunter, C. A. 2005. New IL-12-family members: IL-23 and IL-27, cytokines with divergent functions. *Nat. Rev. Immunol.* 5: 521–531.
43. Koenders, M. I., J. K. Kolls, B. Oppers-Walgreen, L. van den Bersselaar, L. A. Joosten, J. R. Schurr, P. Schwarzenberger, W. B. van den Berg, and E. Lubberts. 2005. Interleukin-17 receptor deficiency results in impaired synovial expression of interleukin-1 and matrix metalloproteinases 3, 9, and 13 and prevents cartilage destruction during chronic reactivated streptococcal cell wall-induced arthritis. *Arthritis Rheum.* 52: 3239–3247.
44. Fujino, S., A. Andoh, S. Bamba, A. Ogawa, K. Hata, Y. Araki, T. Bamba, and Y. Fujiyama. 2003. Increased expression of interleukin 17 in inflammatory bowel disease. *Gut* 52: 65–70.
45. Haznedaroglu, S., M. A. Ozturk, B. Sancak, B. Goker, A. M. Onat, N. Bukan, I. Ertenli, S. Kiraz, and M. Calguneri. 2005. Serum interleukin 17 and interleukin 18 levels in familial Mediterranean fever. *Clin. Exp. Rheumatol.* 23: S77–S80.
46. Sohn, M. H., S. Y. Noh, W. Chang, K. M. Shin, and D. S. Kim. 2003. Circulating interleukin 17 is increased in the acute stage of Kawasaki disease. *Scand. J. Rheumatol.* 32: 364–366.

Research article

Open Access

Arthritogenic T cell epitope in glucose-6-phosphate isomerase-induced arthritis

Keiichi Iwanami[1], Isao Matsumoto[2], Yoko Tanaka[1], Asuka Inoue[1], Daisuke Goto[1], Satoshi Ito[1], Akito Tsutsumi[1] and Takayuki Sumida[1]

[1]Department of Clinical Immunology, Doctoral Program in Clinical Sciences, Graduate School of Comprehensive Human Science, University of Tsukuba, 1-1-1 Tennoudai, Tsukuba 305-8575, Japan
[2]PRESTO, Japan Science and Technology Agency, 4-1-8 Honcho Kawaguchi, Saitama 332-0012, Japan

Corresponding author: Isao Matsumoto, ismatsu@md.tsukuba.ac.jp

Received: 25 Jul 2008 Revisions requested: 22 Sep 2008 Revisions received: 27 Sep 2008 Accepted: 7 Nov 2008 Published: 7 Nov 2008

Arthritis Research & Therapy 2008, **10**:R130 (doi:10.1186/ar2545)
This article is online at: http://arthritis-research.com/content/10/6/R130

Abstract

Introduction Arthritis induced by immunisation with glucose-6-phosphate isomerase (GPI) in DBA/1 mice was proven to be T helper (Th) 17 dependent. We undertook this study to identify GPI-specific T cell epitopes in DBA/1 mice (H-2q) and investigate the mechanisms of arthritis generation.

Methods For epitope mapping, the binding motif of the major histocompatibility complex (MHC) class II (I-Aq) from DBA/1 mice was identified from the amino acid sequence of T cell epitopes and candidate peptides of T cell epitopes in GPI-induced arthritis were synthesised. Human GPI-primed CD4+ T cells and antigen-presenting cells (APCs) were co-cultured with each synthetic peptide and the cytokine production was measured by ELISA to identify the major epitopes. Synthetic peptides were immunised in DBA/1 mice to investigate whether arthritis could be induced by peptides. After immunisation with the major epitope, anti-interleukin (IL) 17 monoclonal antibody (mAb) was injected to monitor arthritis score. To investigate the mechanisms of arthritis induced by a major epitope, cross-reactivity to mouse GPI peptide was analysed by flow cytometry and anti-GPI antibodies were measured by ELISA. Deposition of anti-GPI antibodies on the cartilage surface was detected by immunohistology.

Results We selected 32 types of peptides as core sequences from the human GPI 558 amino acid sequence, which binds the binding motif, and synthesised 25 kinds of 20-mer peptides for screening, each containing the core sequence at its centre. By epitope mapping, human GPI325–339 was found to induce interferon (IFN) γ and IL-17 production most prominently. Immunisation with human GPI325–339 could induce polyarthritis similar to arthritis induced by human GPI protein, and administration of anti-IL-17 mAb significantly ameliorated arthritis ($p < 0.01$). Th17 cells primed with human GPI325–339 cross-reacted with mouse GPI325–339, and led B cells to produce anti-mouse GPI antibodies, which were deposited on cartilage surface.

Conclusions Human GPI325–339 was identified as a major epitope in GPI-induced arthritis, and proved to have the potential to induce polyarthritis. Understanding the pathological mechanism of arthritis induced by an immune reaction to a single short peptide could help elucidate the pathogenic mechanisms of autoimmune arthritis.

Introduction

Rheumatoid arthritis (RA) is characterised by symmetrical polyarthritis and joint destruction. Although the aetiology is considered to be autoimmune reactivity to some antigens, the exact mechanisms are not fully understood. So far, several models of arthritis have been described and analysed to understand the aetiological mechanisms of RA. Glucose-6-phosphate isomerase (GPI)-induced arthritis, a murine model of RA, is induced by immunisation with recombinant human (rh) GPI of DBA/1 mice [1]. We have previously demonstrated

APC: antigen-presenting cell; CIA: collagen-induced arthritis; CII: type II collagen; CTLA-4 Ig: cytotoxic T-lymphocyte antigen 4 immunoglobulin; DAPI: 4',6-diamidino-2-phenylindole, dilactate; ELISA: enzyme-linked immunosorbent assay; FCS: fetal calf serum; GPI: glucose-6-phosphate isomerase; IFN: interferon; IL: interleukin; mAb: monoclonal antibody; MHC: major histocompatibility complex; PBS: phosphate-buffered saline; RA: rheumatoid arthritis; rh: recombinant human; SD: standard deviation; SEM: standard error of the mean; TCR: T cell receptor; Th: T helper.

that the T helper (Th) 17 subset of CD4+ T cells play a central role in the pathogenesis of GPI-induced arthritis; GPI-specific CD4+ T cells were skewed to Th17 at the time of onset, and blockade of interleukin (IL) 17 resulted in a significant amelioration of arthritis [2]. Furthermore, the data that the administration of cytotoxic T-lymphocyte antigen 4 immunoglobulin (CTLA-4 Ig) in the effector phase ameliorated the progress of arthritis implies the importance of Th17 cells even in the effector phase [3].

In this study, we further explored the epitopes of GPI-specific CD4+ T cells and identified human GPI $(hGPI)_{325-339}$ as a major epitope. Interestingly, the amino acid sequence of $hGPI_{325-339}$ (IWYINCFGCETHAML) was the same as that of bovine (type II collagen) $CII_{256-270}$(GEPGIAGFKGEQGPK), the dominant epitope of collagen-induced arthritis (CIA), at the major histocompatibility complex (MHC) binding sites [4]. Of note is that arthritis similar to GPI-induced arthritis was generated by immunisation with a short 15-mer single peptide in genetically unaltered mice. By analysis of peptide-induced arthritis, we found that $hGPI_{325-339}$-primed Th17 cells reacted with mouse GPI $(mGPI)_{325-339}$ peptide and subsequently lead to the production of anti-mouse GPI antibodies, which deposited over the cartilage surface of inflaming joints. Our findings should be helpful in unravelling the mechanism of autoimmune arthritis.

Materials and methods

Mice

DBA/1 mice were purchased from Charles River Laboratories, Japan. All mice were kept under specific pathogen-free conditions and all experiments were conducted in accordance with the University of Tsukuba ethical guidelines.

GPI and synthetic peptides

Recombinant mouse GPI and rhGPI were prepared as described previously [5,6]. Briefly, human GPI or mouse GPI cDNA was inserted into the plasmid pGEX-4T3 (Pharmacia, Uppsala, Sweden) for expression of glutathione S-transferase-tagged proteins. *Escherichia coli* harboring the pGEX-hGPI plasmid was allowed to proliferate at 37°C, before 0.1 mM isopropyl-β-D-thiogalactopyranoside was added to the medium, followed by further culture overnight at 30°C. The bacteria were lysed with a sonicator and the supernatant was purified with a glutathione-sepharose column (Pharmacia, Uppsala, Sweden). The purity was estimated by SDS-PAGE.

Crude peptides were synthesised for epitope screening by Mimotopes (Melbourne, Victoria, Australia), and peptides with 90% purity were synthesised for a major epitope decision and induction of arthritis by Invitrogen (Carlsbad, CA). Candidate peptides, which were thought to bind the binding motif, were selected with web soft MHCPred (The Jenner Institute, Oxford, UK) [7].

Induction of arthritis

DBA/1 mice were immunised with 300 μg rhGPI for GPI-induced arthritis, or 10 μg or 25 μg synthetic peptide for peptide-induced arthritis in complete Freund's adjuvant (Difco Laboratories, Detroit, MI). The rhGPI and synthetic peptide were emulsified with complete Freund's adjuvant at a 1:1 ratio (v/v). For induction of arthritis, 150 μl of the emulsion was injected intradermally at the base of the tail of the mouse. On days 0 and 2 after immunisation, 200 ng of pertussis toxin was injected intraperitoneally to develop peptide-induced arthritis. The arthritis score was evaluated visually using a score of 0 to 3 for each paw. A score of 0 represented no evidence of inflammation, 1 represented subtle inflammation or localised oedema, 2 represented easily identified swelling but localised to either the dorsal or ventral surface of the paws, and 3 represented swelling in all areas of the paws.

Treatments of arthritis with anti-IL-17 monoclonal antibodies

To neutralise IL-17, mice were injected intraperitoneally with 100 μg of neutralising antibody or isotype control on day 7 or day 6, 8, and 10. Anti-IL-17 mAb MAB421 (IgG2a) was purchased from R&D Systems (Minneapolis, MN, USA). IgG2a isotype control was purchased from eBioscience (San Diego, CA, USA).

Analysis of cytokine production

Mice were sacrificed on the indicated day. Spleens were harvested and haemolysed with a solution of 0.83% NH_4Cl, 0.12% $NaHCO_3$ and 0.004% $EDTA_2Na$ in PBS. Single-cell suspensions were prepared in RPMI1640 medium (Sigma-Aldrich, St. Louis, MO) containing 10% FCS, 100 U/ml of penicillin, 100 μg/ml of streptomycin and 50 μM 2-mercaptoethanol. CD4+ T cells were isolated by MACS positive selection (Miltenyi Biotec, Bergisch Gladbach, Germany). The purity of the collected cells (>97%) was confirmed by flow cytometry. Splenic feeder cells treated with 50 μg/ml of mitomycin C were used as antigen presenting cells (APCs). The purified CD4+ T cells and APCs were co-cultured with 10 μM of the synthetic peptide at a ratio of 5:1 at 37°C under 5% CO_2 for 24 hours. The supernatants were assayed for interferon (IFN)-γ and IL-17 by Quantikine ELISA kit (R&D Systems, Minneapolis, MN).

Intracellular cytokine staining and flow cytometric analysis

Mice were sacrificed on day 5. The draining lymph nodes were harvested and single cell suspensions were prepared as described above. Cells (1×10^6/ml) were stimulated with 10 μM of the synthetic peptides in 96-well round bottom plates (Nunc, Roskilde, Denmark) for 24 hours and GoldiStop (BD PharMingen, San Diego, CA) was added for the last four hours of each culture. Cells were first stained extracellularly, fixed and permeabilised with Cytofix/Cytoperm solution (BD PharMingen, San Diego, CA) and then stained intracellularly.

Samples were acquired on FACSCalibur (BD PharMingen, San Diego, CA) and data were analysed with FlowJo (Tree Star, Ashland, OR).

Analysis of anti-GPI antibody

Sera were taken from immunised mice on day 14 and diluted 1:500 in blocking solution (25% Block Ace (Dainippon Sumitomo Pharma, Osaka, Japan) in PBS) for antibody analysis. We also prepared 96-well plates (Sumitomo Bakelite, Tokyo, Japan) coated with 5 μg/ml rhGPI or recombinant mouse GPI for 12 hours at 4°C. After washing twice with a washing buffer (0.05% Tween20 in PBS), the blocking solution was used for blocking nonspecific binding for two hours at room temperature. After three washes, 150 μl of the diluted serum was added and incubated for two hoursat room temperature. After three washes, alkaline phosphatase-conjugated anti-mouse IgG was added at a final dilution of 1:5000, for one hour at room temperature. After three washes, colour was developed with substrate solution (1 alkaline phosphatase tablet (Sigma-Aldrich, St. Louis, MO, USA) per 5 ml alkaline phosphatase reaction solution (containing 9.6% diethanolamine and 0.25 mM $MgCl_2$, pH 9.8)). Plates were incubated for 20 minutes at room temperature and optical density was measured by a microplate reader at 405 nm.

Immunohistology

For immunohistology, cryostat sections from ankle joints were prepared with the tape capture technique as described previously [8]. Briefly, ankle joints were taken from immunised mice on day 14 and placed in Tissue-Tek (Sakura Finetek, Torrance, CA) filled with 4% carboxymethyl cellulose compound (Finetec, Tokyo, Japan). Frozen ankles joints in the carboxymethyl cellulose compound were attached to the adhesive Cryofilm (Finetec, Tokyo, Japan) and were cut in the microtome. The sections on the adhesive film were fixed with cold acetone. After blocking with 2% bovine serum albumin and 0.05% Tween in PBS, the sections were stained with Alexa 546-conjugated anti-mouse IgG (Invitrogen, Carlsbad, CA) (200 ng/slide), and nuclei were counterstained with 4',6-diamidino-2-phenyindole dilactate (DAPI) (Sigma-Aldrich, St. Louis, MO, USA) (50 ng/slide). Fluorescence was detected with the Leica DMRA2 microscopy (Leica, Wetzlar, Germany). The images were acquired and processed with Leica FW4000 (Leica, Wetzlar, Germany).

Statistical analysis

All data were expressed as mean ± standard error of the mean (SEM) or standard deviation (SD). Differences between groups and variables were examined for statistical significance using the Mann-Whitney's U test and the Spearman's rank correlation coefficient, respectively. A $p < 0.05$ denoted the presence of a statistically significant difference.

Results

I-A^q binding motif and epitope candidates

To analyse T cell epitopes, we first investigated the binding motif of I-A^q from T cell epitopes reported in the literature because DBA/1 mice express only I-A^q as MHC class II. Based on the work by Bayrak and colleagues [9], the anchor motif of I-A^q would exist at P1, P4 and P7, therefore we predicted the binding motifs from amino acid sequences of I-A^q restricted epitopes on murine $RNase_{90-105}$ [10], myelin basic $protein_{89-101}$ [11,12], chicken type II collagen $(CII)_{181-209}$ [13], rat $CII_{256-270}$ [14,15], bovine $CII_{256-270}$ [4] and mouse type II collagen [9] (Table 1). Next, we selected 32 types of peptides as core sequences from the human GPI 558 amino acid sequence, which is thought to bind the binding motif (Table 2), and synthesised 25 kinds of 20-mer peptides for screening, each containing the core sequence in its centre (Table 3).

Epitope screening

rhGPI-specific CD4$^+$ T cells differentiate into Th1 and Th17 [2], so we analysed IFN-γ and IL-17 production for epitope screening when rhGPI-primed CD4$^+$ T cells were stimulated with each synthetic peptide. The production of both IFN-γ and IL-17 was pronounced when GPI-primed CD4$^+$ T cells were stimulated with number 18 peptide ($hGPI_{327-346}$) and number 25 peptide ($hGPI_{539-558}$). Therefore, we considered that major epitopes exist in either of the two peptides (Figure 1). In the K/BxN mouse model of arthritis, KRN T cell receptor (TCR) transgenic T cells recognise $mGPI_{282-294}$, the dominant epitope of K/BxN mouse, on I-A^{g7} [16]. However, in the GPI-induced arthritis model, it was unlikely that $hGPI_{282-294}$ was the dominant epitope because GPI-specific T cells did not react prominently to number 16 peptide ($hGPI_{280-299}$).

Because the synthetic peptides used for screening were not purified, we re-synthesised the 15-mer peptides with a purity of 90%; these peptides contained each core sequence of

Table 1

I-Aq binding motifs

P1	P2	P3	P4	P5	P6	P7	P8	P9
A			A			E		
F			P			D		
L			F			Q		
I			S			P		
P			V			N		
S			L			I		
V			N					
			R					

The anchor motif of I-A^q would exist at P1, P4 and P7, therefore we predicted the binding motif from amino acid sequences of I-A^q restricted epitopes on murine $RNase_{90-105}$, myelin basic $protein_{89-101}$, chicken type II $collagen_{181-209}$, rat type II $collagen_{256-270}$, bovine type II $collagen_{256-270}$ and mouse type II collagen.

Table 2

Core sequences of glucose-6-phosphate isomerase (GPI) amino acids binding I-A^q

Peptide	Amino acid residues
3–11	ALTRDPQFQ
29–37	LFDANKDRF
41–49	SLTLNTNHG
56–64	SKNLVTEDV
72–80	AKSRGVEAA
80–88	ARERMFNGE
99–107	LHVALRNRS
102–110	ALRNRSNTP
149–157	ITDVINIGI
167–175	VTEALKPYS
173–181	PYSSGGPRV
181–189	VWYVSNIDG
196–204	LAQLNPESS
201–209	PESSLFIIA
210–218	SKTFTTQET
229–237	FLQAAKDPS
230–238	LQAAKDPSA
243–251	FVALSTNTT
253–261	VKEFGIDPQ
285–293	ALHVGFDNF
319–327	LLALLGIWY
328–336	INCFGCETH
337–345	AMLPYDQYL
391–399	FYQLIHQGT
403–411	PCDFLIPVQ
407–415	LIPVQTQHP
426–434	LANFLAQTE
452–460	AGKSPEDLE
489–497	ALVAMYEHK
537–545	SHDASTNGL
540–548	ASTNGLINF
545–553	LINFIKQQR

Thirty-two types of peptides were selected as core sequences from the GPI 558 amino acid sequence, which is thought to bind the binding motif. Amino acid residues that are thought to bind anchors of I-A^q are shown in bold letters.

number 18 peptide ($hGPI_{327-346}$) and number 25 peptide ($hGPI_{539-558}$). Number 18 peptide ($hGPI_{327-346}$) contains two core sequences ($hGPI_{328-336}$ and $hGPI_{337-345}$), so therefore we re-synthesised two peptides ($hGPI_{325-339}$ and $hGPI_{334-348}$). The former sequences of number 25 peptide ($hGPI_{539-558}$) overlapped with number 24 peptide ($hGPI_{533-552}$), which could not stimulate CD4$^+$ T cells primed with GPI. Therefore we re-synthesised two peptides ($hGPI_{542-556}$ and $hGPI_{544-558}$) from the latter sequences of number 25 peptide (Table 4). We analysed IFN-γ and IL-17 production for epitope screening as described above. The peptide ($hGPI_{325-339}$) induced marked stimulation of GPI-primed CD4$^+$ T cells, and was considered a major epitope (Figure 2).

Immunisation with a major epitope induces arthritis similar to GPI-induced arthritis

To test if $hGPI_{325-339}$ is arthritogenic, DBA/1 mice were immunised with 10 μg or 25 μg $hGPI_{325-339}$ instead of GPI protein, and 200 ng of pertussis toxin was injected intraperitoneally on days 0 and 2 after immunisation. Arthritis resembling GPI-induced arthritis could be generated by immunisation with the peptide, including incidence, manifestations and severity. Symmetrical polyarthritis appeared on day 8, showed peak severity on day 14 and subsided gradually thereafter (Figure 3a). The use of different immunisation doses (10 and 25 μg) did not seem to affect the incidence and severity of arthritis. Immunised with 10 μg or 25 μg $hGPI_{325-339}$ without injection of pertussis toxin could also induce arthritis. However, the arthritis was less severe than with pertussis toxin (data not shown). On the other hand, immunisation with neither $hGPI_{539-558}$ nor $hGPI_{544-558}$, which were considered minor epitopes in GPI-induced arthritis, could induce overt arthritis (Figure 3a). Mice immunised with $hGPI_{325-339}$ developed severe swelling of the wrist and ankle joints. Histologically, severe synovitis was noted in the wrists in the forepaws, and at ankles and tarsal joints in the hind paws (Figure 3b and data not shown).

Peptide-induced arthritis is mediated by Th17

GPI-induced arthritis is Th17-mediated [2], so we explored the aetiological role of Th17 in peptide-induced arthritis. Like GPI-induced arthritis, one time administration of anti-IL-17 mAb on day 7 and three times administration on day 6, 8 and 10 significantly ameliorated the arthritis (Figure 4). From these data, the arthritis induced by $hGPI_{325-339}$ was also considered to be Th17 mediated.

Immunisation of human $GPI_{325-339}$ leads Th17 cells to cross-react with mouse $GPI_{325-339}$

We examined the pathogenesis of arthritis induced by $hGPI_{325-339}$ by comparing it with mice immunised with $hGPI_{544-558}$.

First, we speculated that the difference in cross-reactivity to mouse GPI might affect the incidence of arthritis, because $hGPI_{325-339}$ (IWYINCFGCETHAML) has 13/15 amino acids homology to $mGPI_{325-339}$ (IWYINCYGCETHALL) while $hGPI_{544-558}$ (GLINFIKQQREARVQ) has only 9/15 amino

Table 3

Synthetic peptides for screening T cell epitopes

Peptide number	Peptide	Synthetic peptide sequence
1	1–20	H-MA**A**LT**R**DP**Q**F**Q**KLQQWYREH-OH
2	23–42	H-ELNLRR**L**FD**A**NK**D**RFNHFSL-OH
3	37–56	H-FNHF**S**LTLNT**N**H**G**HILVDYS-OH
4	51–70	H-ILVDY**S**KNL**V**T**E**DVMRMLVD-OH
5	71–90	H-L**A**KS**R**GV**E**A**A**RER**M**F**N**GEKI-OH
6	96–115	H-RAV**L**H**V**AL**R**N**R**S**N**T**P**ILVDG-OH
7	145–164	H-TGKT**I**TD**V**IN**I**G**I**GGSDLGP-OH
8	162–181	H-LGPLM**V**T**E**AL**K**PY**S**SGGPRV-OH
9	168–187	H-TEALK**P**Y**S**S**G**G**P**R**V**WYVSNI-OH
10	176–195	H-SGGPR**V**W**Y**V**S**N**I**DGTHIAKT-OH
11	191–210	H-HIAKT**L**AQ**L**N**P**E**S**SLFIIAS-OH
12	200–219	H-N**P**E**S**S**L**FIIA**S**K**T**F**T**T**Q**ETI-OH
13	225–244	H-AKEW**F**L**Q**A**A**K**D**P**S**AVAKHFV-OH
14	238–257	H-AVAKH**F**V**A**LS**T**N**T**TKVKEFG-OH
15	247–266	H-STNTTK**V**K**E**FG**I**D**P**QNMFEF-OH
16	280–299	H-IGLSI**A**LH**V**GF**D**NFEQLLSG-OH
17	313–332	H-EKNAPV**L**LA**L**LG**I**W**Y**INCFG-OH
18	327–346	H-Y**I**NC**F**G**C**E**T**H**A**ML**P**YD**Q**YLH-OH
19	386–405	H-NGQHA**F**YQ**L**IH**Q**G**T**KMIPCD-OH
20	400–419	H-KMI**P**C**D**F**L**IP**V**QT**Q**H**P**IRKG-OH
21	420–439	H-LHHKIL**L**AN**F**LA**Q**TEALMRG-OH
22	445–464	H-ARKELQA**A**GK**S**PE**D**LERLLP-OH
23	484–503	H-PFMLG**A**LV**A**MY**E**H**K**IFVQGI-OH
24	533–552	H-AQVT**S**HD**A**ST**N**GLINFIKQQ-OH
25	539–558	H-DASTNG**L**INF**I**K**Q**QR**E**ARVQ-OH

Listed are 25 20-mer unpurified peptides in which each core sequence were centred around. Amino acid residues constituting the core sequence and those thought to bind anchors of I-A^q are underlined and shown in bold letters, respectively.

acids homology to $mGPI_{544-558}$ (GLISFIKQQRDTKLE). The draining lymph node cells from mice immunised with $hGPI_{325-339}$ or $hGPI_{544-558}$were cultured in the presence of $hGPI_{325-339}$, $mGPI_{325-339}$, $hGPI_{544-558}$ or $mGPI_{544-558}$ for 24 hours. The $hGPI_{325-339}$-primed cells had distinct cross-reactive immune reaction to $mGPI_{325-339}$ by producing IL-17, whereas the $hGPI_{544-558}$ primed cells did not cross-react to $mGPI_{544-558}$ (Figure 5a). As compared with the draining lymph node cells of $hGPI_{325-339}$-immunised mice, IL-17 production was not remarkable in that of $hGPI_{544-558}$-immunised mice even when the corresponding peptide was used as an antigen for *in vitro* stimulation (Figure 5a). The production of IFN-γ was much lower than that of IL-17, and IL-4 production was not detectable independent of immunisation patterns and antigens for *in vitro* stimulation (data not shown).

It has been reported that Th17 cells are not the only cellular sources of IL-17, but $CD8^+$ T cells, natural killer T cells and γδT cells are also capable of producing IL-17 [17-22]. Therefore, we investigated the IL-17 producing cells using flow cytometry. The draining lymph node cells from mice immunised with $hGPI_{325-339}$ or $hGPI_{544-558}$ were stimulated with $hGPI_{325-339}$ and $mGPI_{325-339}$, or $hGPI_{544-558}$ and $mGPI_{544-558}$, respectively. Intracellular cytokine staining was performed without nonspecific stimulants, such as phorbol myristate acetate or ionomycin. We confirmed that immunisation of $hGPI_{325-339}$ induced antigen-specific Th17 cells, which cross-reacted with $mGPI_{325-339}$. However, immunisation of $hGPI_{544-558}$ induced neither $hGPI_{544-558}$-specific Th17 cells nor Th17 cells that can cross-react with $mGPI_{544-558}$ remarkably (Figure 5b). These data indicate that induction of antigen-specific Th17 cells and

Figure 1

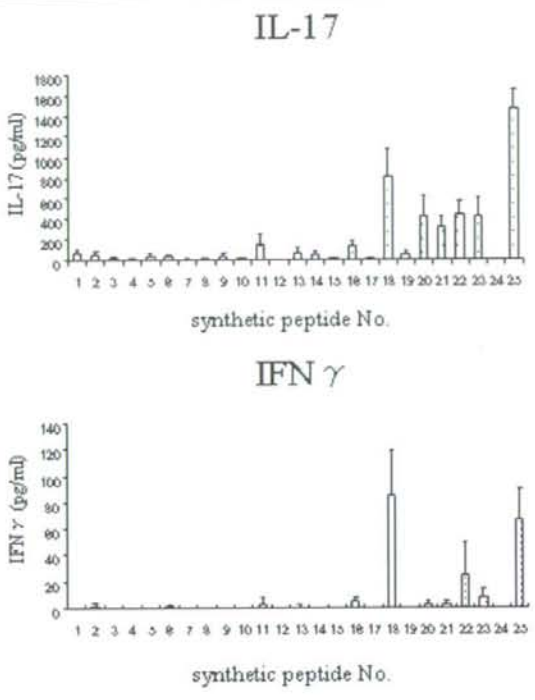

Synthetic peptides number 18 and 25 produced marked simulation of glucose-6-phosphate isomerase (GPI) primed CD4+ T cells. Mice were sacrificed on day 7 after immunisation. CD4+ T cells were purified from spleen cells of GPI-immunised DBA/1 mice. GPI-primed CD4+ T cells and antigen presenting cells (APCs) were co-cultured with 10 μM of synthetic peptide for 24 hours. The supernatants were assayed for interferon (IFN) γ and interleukin (IL) 17 by ELISA. Data are averages ± standard deviation of three culture wells. Representative data of three independent experiments.

cross-reactivity with mouse GPI might be the pathogenesis of peptide-induced arthritis.

Immunisation of human $GPI_{325-339}$ leads B cells to produce anti-mouse GPI antibodies

To explore the importance of autoantibodies, we measured anti-human GPI antibodies and anti-mouse GPI antibodies in mice immunised with $hGPI_{325-339}$, $hGPI_{544-558}$ and $hGPI_{325-339}$ plus $hGPI_{544-558}$ by ELISA. Mice immunised with rhGPI and the two peptides ($hGPI_{325-339}$ plus $hGPI_{544-558}$) produced high titres of anti-human GPI antibodies and anti-mouse GPI antibodies, and mice immunised with $hGPI_{325-339}$ and $hGPI_{544-558}$ hardly produced any anti-human GPI antibodies. However, mice immunised with $hGPI_{325-339}$ produced significantly higher titres of anti-mouse GPI antibodies than mice immunised with $hGPI_{544-558}$ (Figure 6a). It is noteworthy that immunisation with the two peptides ($hGPI_{325-339}$ plus $hGPI_{544-558}$) induced significantly higher titres of anti-mouse

Figure 2

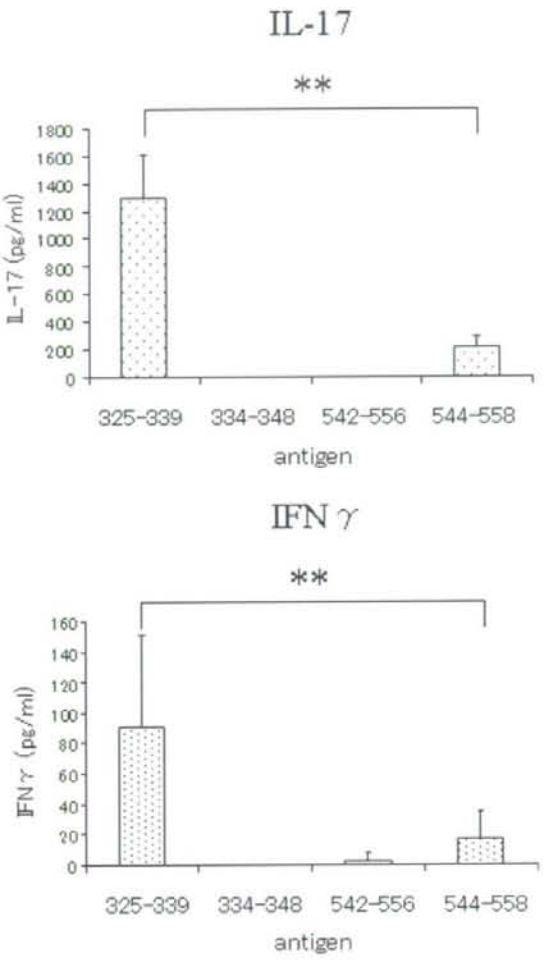

$GPI_{325-339}$ is a major epitope. Mice were sacrificed on day 7 after immunisation. CD4+ T cells were purified from splenocytes of glucose-6-phosphate isomerase (GPI) immunised DBA/1 mice. GPI-primed CD4+ T cells and antigen presenting cells (APCs) were co-cultured with 10 μM of synthetic peptide $hGPI_{325-339}$, $hGPI_{334-348}$, $hGPI_{542-556}$ or $hGPI_{544-558}$ for 24 hours. The purity of each peptide was 90%. The supernatants were assayed for interferon (IFN) γ and interleukin (IL) 17 by ELISA. Data are averages ± standard deviation of five culture-wells. **$p < 0.01$ (Mann-Whitney's U test). Representative data of three independent experiments.

GPI antibodies than that with $hGPI_{325-339}$ alone, whereas the severity and incidence of arthritis in mice immunised with two peptides ($hGPI_{325-339}$ plus $hGPI_{544-558}$) were comparable with those in mice immunised with $hGPI_{325-339}$ alone (Figures 3a and 6a).

Table 4

Re-synthesised peptides used for determining a major epitope

Peptide number	Peptide	Synthetic peptide sequence
18	327–346	H-YINCFGCETHAMLPYDQYLH-OH
	325–339	H-IWYINCFGCETHAML-OH
	334–348	H-ETHAMLPYDQYLHRF-OH
25	539–558	H-DASTNGLINFIKQQREARVQ-OH
	542–556	H-TNGLINFIKQQREAR-OH
	544–558	H-GLINFIKQQREARVQ-OH

The 15-mer peptides were synthesised with 90% purity, containing each core sequence of number 18 peptide ($GPI_{327-346}$) and number 25 peptide ($GPI_{539-558}$). Amino acid residues constituting the core sequence and those thought to bind the anchors of I-A^q are underlined and shown in bold letters, respectively.

We further investigated the difference of the correlation between anti-mouse GPI antibodies and arthritis score among immunisation patterns. Each of the three different immunisation patterns (rhGPI, $hGPI_{325-339}$ and $hGPI_{325-339}$ plus $hGPI_{544-558}$) showed no positive correlation between anti-mouse GPI antibodies and arthritis score (Table 5).

Next, we investigated the existence of IgG on the cartilage surface by immunohistology, because GPI were proved to deposit on the cartilage surface of normal naïve mice [23]. The cryostat sections of ankle joints from naïve mice and mice immunised with $hGPI_{544-558}$ did not show IgG deposit on the cartilage surface. However, those from mice immunised with rhGPI and $hGPI_{325-339}$ showed IgG deposits (Figure 6b). These data indicate that anti-mouse GPI antibodies may play a role in the development of peptide-induced arthritis.

Discussion

GPI, a ubiquitous glycolytic enzyme, is a new autoantigen candidate in autoimmune arthritis [5,6]. GPI-induced arthritis is induced by immunisation of genetically unaltered DBA/1 mice with rhGPI [1]. We report here the therapeutic efficacies of mAb to tumour necrosis factor-α and IL-6 and CTLA-4 Ig in this model [3]. Moreover, $CD4^+$ T cells, especially Th17 cells, seem to be more important than B cells, because administration of anti-CD4 mAb or anti-IL-17 mAb markedly ameliorate the progress of arthritis independent of anti-GPI antibodies titres [1,2]. Therefore, exploring the epitope of $CD4^+$ T cells and its arthritogenic effect is important for understanding the pathological mechanisms.

In this study, we investigated the binding motif of I-A^q from T cell epitopes considered to bind to I-A^q, synthesised peptides of epitope candidates and identified $hGPI_{325-339}$ as a major epitope. Interestingly, the MHC binding residues of $hGPI_{325-339}$(IWYINCFGCETHAML) at P1, P4 and P7 were the same as those for bovine $CII_{256-270}$ (GEP-

Figure 3

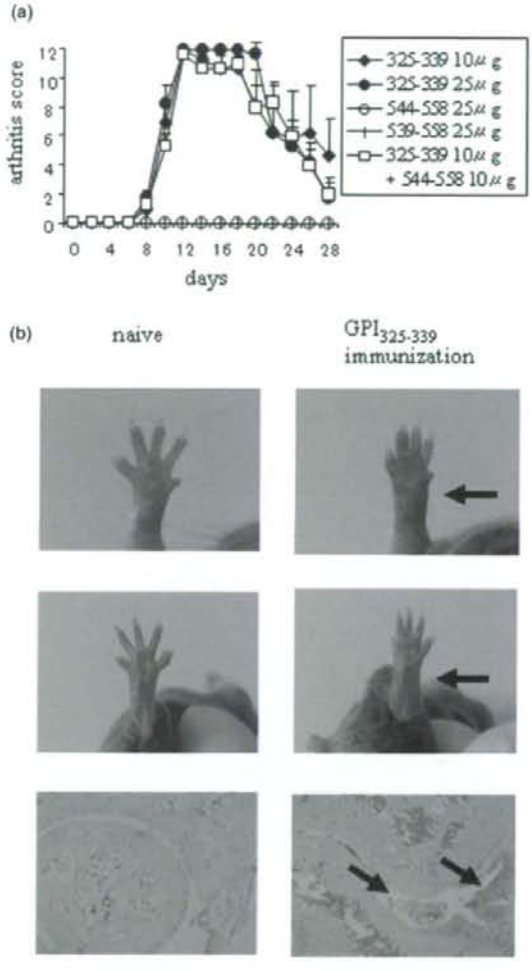

Immunisation with $hGPI_{325-339}$ induces severe polyarthritis. DBA/1 mice were immunised with 25 μg of $hGPI_{325-339}$, $hGPI_{539-558}$ or $hGPI_{544-558}$, or 10 μg each of $hGPI_{325-339}$ plus $hGPI_{544-558}$, and 200 ng of pertussis toxin was injected intraperitoneally on days 0 and 2 after immunisation. (a) The mean arthritis score (± standard error of the mean (SEM)) of five mice in one representative experiment of two independent experiments. (b) Severe swelling of the wrist (upper panels) and ankle joints (middle panels) in mice immunised with 25 μg of $hGPI_{325-339}$ compared with naïve mice (arrowheads). Histological analysis of haematoxylin & eosin-stained sections of ankle joints taken from naïve mice and mice on day 14 after $hGPI_{325-339}$ immunization (lower panels) showed severe synovitis with massive infiltration of cells and hyperplasia of synovial tissue (arrowheads).

induced arthritis [4]. These findings indicate that the binding motif (P1 I, P4 F, P7 E) might have high binding affinity with I-A^q, and the peptides with this motif-MHC complexes might be effectively recognised by TCRs and could be arthritogenic in some condition. Although immunisation with a fragment of

Figure 4

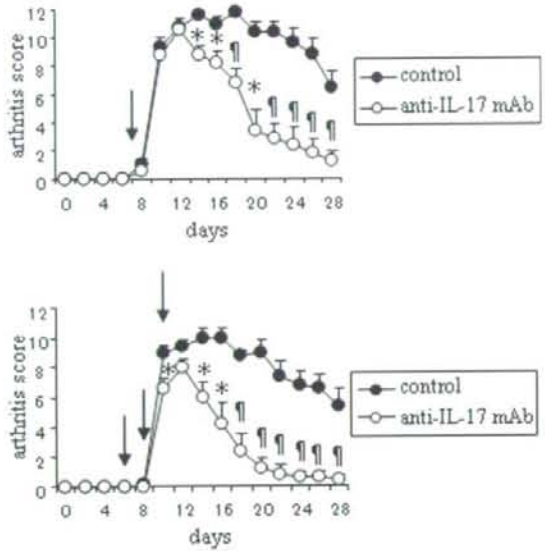

Anti-IL-17 monoclonal antibody (mAb) suppresses the development of arthritis. DBA/1 mice were immunised with 25 μg of $hGPI_{325-339}$, and 200 ng of pertussis toxin was injected intraperitoneally on days 0 and 2 after immunisation. 100 μg of anti-IL-17 mAb or isotype control (control) was administered intraperitoneally on day 7 (upper panel) or day 6, 8, and 10 (lower panel) after immunisation (arrow). Mean arthritis score (± standard error of the mean (SEM)) of five mice per group. Representative data of two independent experiments. * $p < 0.05$, ¶ $p < 0.01$ (Mann-Whitney's U test).

cyanogen bromide of bovine CII, CB11 ($CII_{124-402}$), which contains the dominant epitope, can induce arthritis, the severity and incidence are much lower than arthritis induced by bovine CII protein [4]. Other fragments (CB8, CB9, CB10 and CB12) do not induce arthritis, as is explained by the production of anti-bovine CII antibodies. Immunisation with CB11 fragment produces five times more antibodies to bovine CII than any other fragment [4]. The observation that administration of anti-CD4 mAb after the onset of arthritis did not ameliorate the arthritis [24,25] and a combination of mAb to CII can passively transfer arthritis to naïve mice [26] also emphasises the importance of autoantibodies to the induction of collagen-induced arthritis.

Our study demonstrated that immunisation with $hGPI_{325-339}$ induced antigen-specific Th17 cells, which can cross-react with $mGPI_{325-339}$ and lead B cells to produce anti-mouse GPI antibodies. However, immunisation with $hGPI_{544-558}$ could not even induce $hGPI_{544-558}$-specific Th17 cells. The difference of ability of Th17 induction between two peptides may come from MHC-binding affinity and TCR-binding affinity. A peptide that is likely to bind to MHC class II with high affinity and interacts strongly with the T cell receptor tends to stimulate Th1-cell response, whereas a peptide with low binding affinity to MHC class II and T cell receptor tends to elicit Th2-cell response [27,28]. Although the relationship between Th17 differentiation and the strength of TCR signalling and MHC-binding affinity has not been clarified, it is possible that the difference in amino acid sequences between $hGPI_{325-339}$ and $hGPI_{544-558}$ might affect the I-Aq binding affinity and the TCR signalling, and consequently lead to the difference in extent of antigen-specific Th17 cells. In this study, we did not detect any IL-4 production, which is an adjuvant effect of *Mycobacterim tuberculosis* and pertussis toxin.

In K/BxN mice expressing $I\text{-}A^{g7}$ as MHC class II molecules, $mGPI_{282-294}$-specific $CD4^+$ T cells lead B cells to produce anti-mouse GPI antibodies [16]. The anti-mouse GPI antibodies from K/BxN mice have such high affinity that IgG transfer of K/BxN mice can provoke arthritis in normal mice [6]. In comparison, the anti-mouse GPI antibodies from GPI-induced arthritis alone are not sufficient for the development of arthritis because IgG transfer from mice immunised with rhGPI can not provoke arthritis. However, IgG signalling through FcγR seems necessary for the induction of GPI-induced arthritis because FcγR-deficient mice are resistant to arthritis [1]. Moreover, the data that transfer of rhGPI-primed or $hGPI_{325-339}$-primed Th17 cells to naïve DBA/1 mice can not induce arthritis emphasises the necessity of anti-mouse GPI antibodies (unpublished observation). Considering the data that there are no positive correlation between anti-mouse GPI antibodies and arthritis score [[29] and unpublished observation], and arthritis-resistant mice like C57BL/6 produce as high titres of anti-mouse GPI antibodies as DBA/1 when immunised with rhGPI (1 and unpublished observation), anti-mouse GPI antibodies may play a subordinate role in the development of GPI-induced arthritis and peptide-induced arthritis in DBA/1 mice.

In the process of epitope screening, the response to $hGPI_{539-558}$ peptide was comparable with that to $hGPI_{327-346}$ peptide; however, the response to $hGPI_{542-558}$ and $hGPI_{544-558}$, which were synthesised with 90% purity, was lower than that to $hGPI_{539-558}$ peptide. Furthermore, the response to $hGPI_{539-558}$, which was re-synthesised with 90% purity, was much lower than to $hGPI_{325-339}$ or to $hGPI_{539-558}$ peptide for screening (data not shown). These results could be explained by differences in the purity of the synthetic peptides. The synthetic peptides used for screening (peptides numbers 1 to 25, Table 2) were unpurified, and the purity of each peptide would have been quite different, although the exact purity was unchecked by the product maker. Therefore, it is possible that the purity of number 25 peptide might have been much higher than that of number 18 peptide, or alternatively, number 25 peptide may have contained other peptides through peptide synthesis.

From a probability point of view, it is possible that other epitopes exist in some regions of human GPI-amino acid

Figure 5

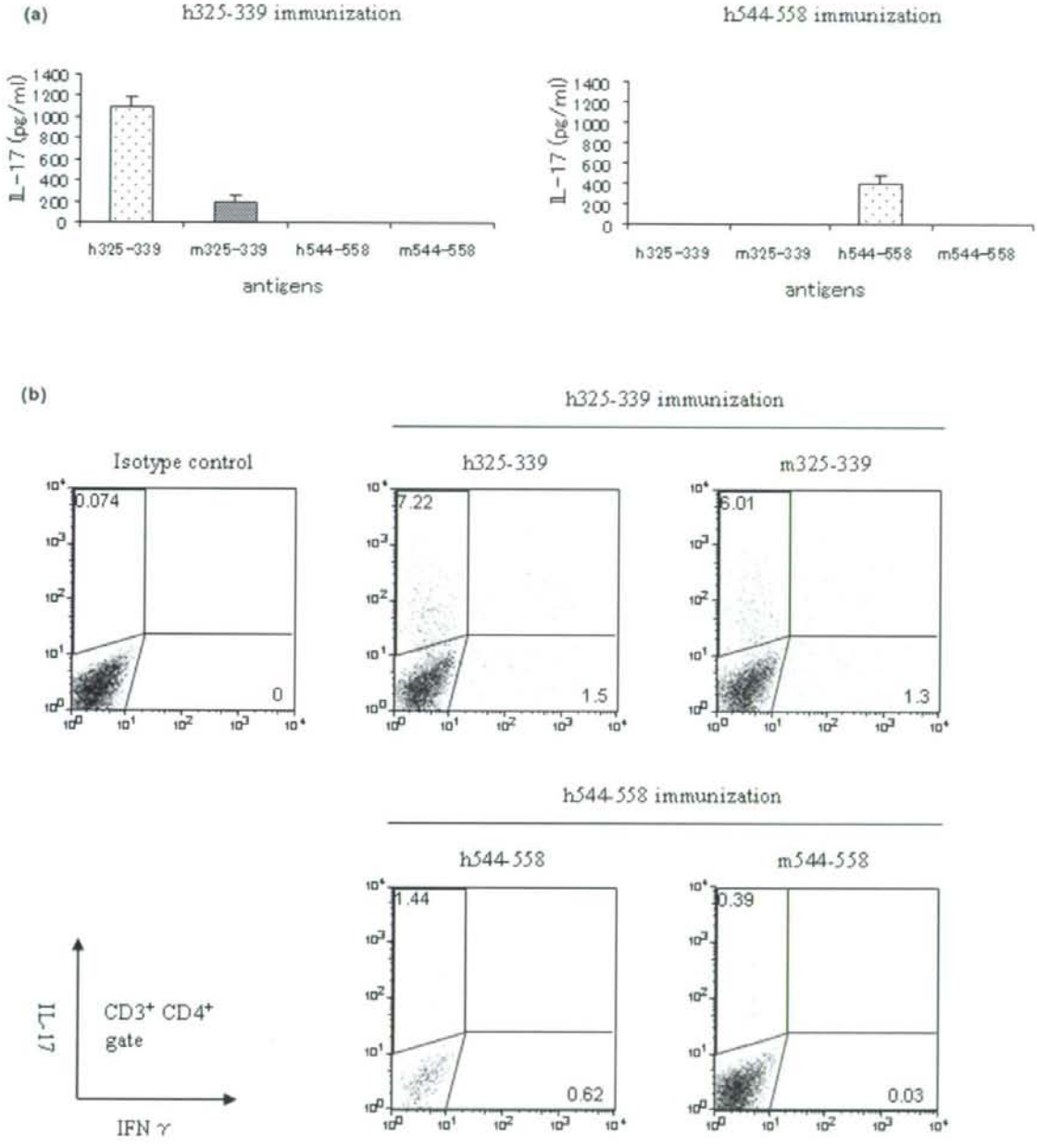

Cross-reactivity with peptides derived from mouse glucose-6-phosphate isomerase (GPI). (a) Draining lymph node (DLN) cells taken from $hGPI_{325-339}$-immunised mice on day 5 were cultured with 10 μM of $hGPI_{325-339}$, $mGPI_{325-339}$, $hGPI_{544-558}$ or $mGPI_{544-558}$ for 24 hours. The supernatants were assayed for interleukin (IL) 17 by ELISA. Data are averages ± standard deviation of three culture-wells. Representative data of three independent experiments. (b) DLN cells taken from $hGPI_{325-339}$- or $hGPI_{544-558}$-immunised mice on day 5 were cultured with 10 μM of $hGPI_{325-339}$ and $mGPI_{325-339}$ or $hGPI_{544-558}$ and $mGPI_{544-558}$, respectively. GoldiStop was added at the last four hours of each culture. Flow cytometry for IL-17 and interferon (IFN) γ was gated in $CD3^+$, $CD4^{high}$ cells. Representative flow cytometry data of three independent experiments with two mice per experiment.

Figure 6

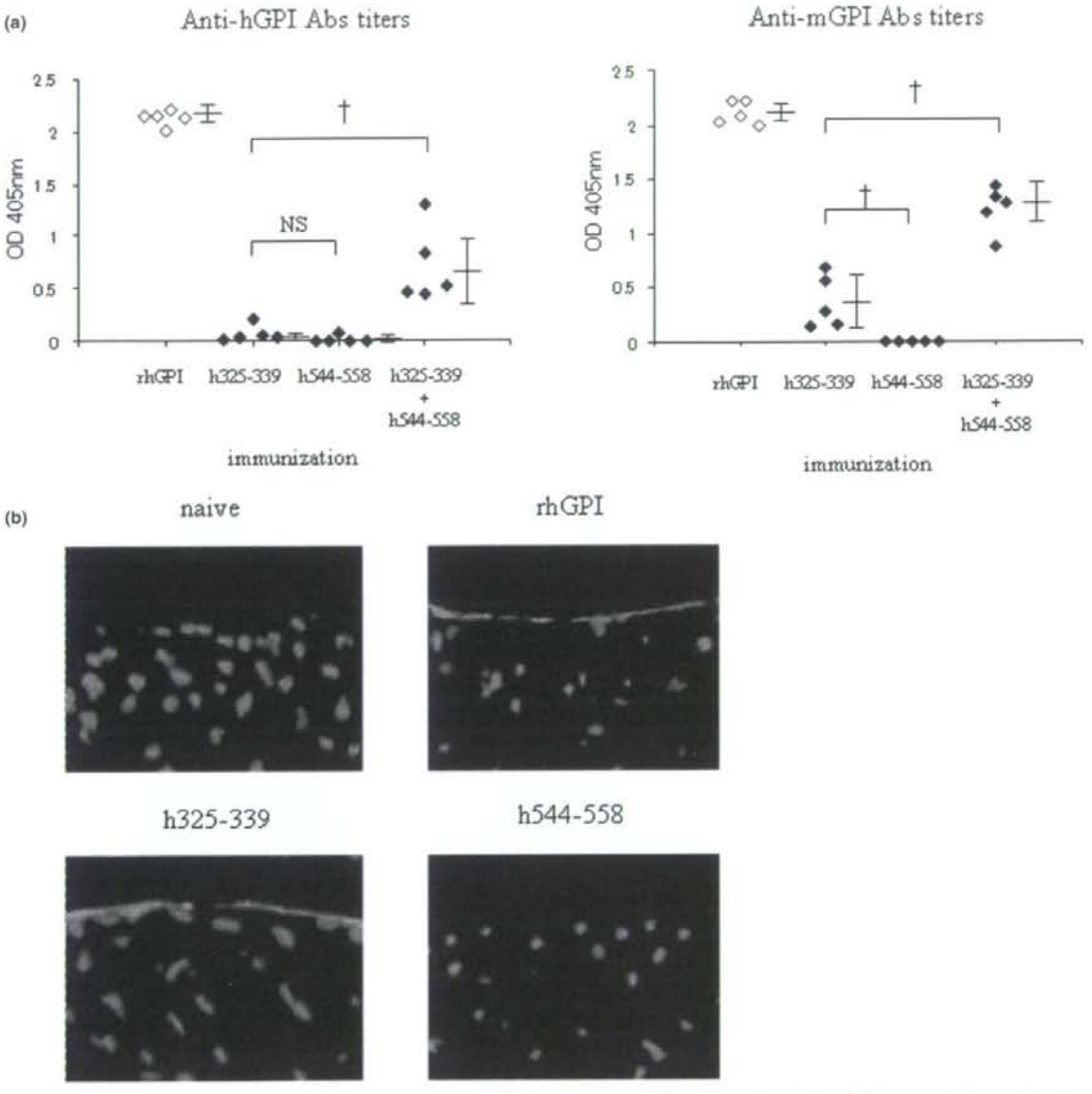

Titres of anti-mouse glucose-6-phosphate isomerase (GPI) antibodies were elevated in mice with arthritis. (a) Sera were taken on day 14 from mice immunised with recombinant human (rh) GPI, $hGPI_{325-339}$, $hGPI_{544-558}$ or $hGPI_{325-339}$ plus $hGPI_{544-558}$, and the titres of anti-human GPI antibodies and anti-mouse GPI antibodies were analysed by ELISA. Each symbol represents a single mouse. Data are mean optimal density ± standard deviation. †$p < 0.01$ (Mann-Whitney's U test). Representative data of two independent experiments. (b) Ankle joints were taken on day 14 from mice immunised with rhGPI, $hGPI_{325-339}$ or $hGPI_{544-558}$. Cryostat sections of ankle joints were stained with anti-mouse IgG (red), and nuclei were counterstained with 4',6-diamidino-2-phenyindole dilactate (blue). Representative data of three independent experiments.

sequence from which we did not synthesise the peptides, because $I\text{-}A^q$ may have another binding motif and our synthesised peptides covered only the 399/558 (71.5%) amino acid residues of human GPI protein, not the whole length. However, two experimental pieces of data support that $hGPI_{325-339}$ may be the dominant epitope. One is that immunisation with $hGPI_{325-339}$ provoked arthritis similar to that induced by rhGPI protein. The other is that intraperitoneal injection of $hGPI_{325-339}$ after the onset of arthritis significantly ameliorated the progress of arthritis (data not shown). Because systemic

Table 5

Correlation between anti-mouse glucose-6-phosphate isomerase (GPI) antibodies titres and arthritis score

Immunisation	Rho value	P value
rhGPI	-0.825	0.0989
h325–339	-0.525	0.2937
h325–339 plus h544–558	0.500	0.3173

Sera were taken on day 14 from mice immunised with recombinant human (rh) GPI, $hGPI_{325-339}$ or $hGPI_{325-339}$ plus $hGPI_{544-558}$. The correlation between the titres of anti-GPI antibodies and arthritis score on day 14 were statistically analysed with the Spearman's rank correlation coefficient. In the case of five samples, Rho values above 0.900 indicate significant positive correlation between anti-mouse GPI antibody titres and arthritis score, whereas Rho values below -0.900 indicate significant negative correlation ($p < 0.05$). Five mice per group. Representative data of two independent experiments.

administration of a dominant epitope leads to anergy of pathogenic T cells or results in activation-induced cell death [30,31], this inhibitory effect of $hGPI_{325-339}$ on GPI-induced arthritis supports the notion that $hGPI_{325-339}$ may be the dominant epitope.

Cross-reactivity is considered the one of mechanisms of autoimmune diseases. We previously identified patients with RA who have GPI-reactive $CD4^+$ T cells and found that some of them express human leucocyte antigen-DR4 as MHC class II [32]. Because the $I\text{-}A^q$ binding motif resembles DR4 [9], further studies are needed to define epitopes of $CD4^+$ T cells in such patients and search proteins that have homology to the epitopes.

Conclusions

This study is the first report of experimental arthritis induced by immunisation with a single short peptide in genetically unaltered mice. The fact that an immunological reaction to a single short peptide of ubiquitously expressed protein causes polyarthritis provides new insight to the understanding of autoimmune arthritis.

Competing interests

The authors declare that they have no competing interests.

Authors' contributions

KI wrote the manuscript and conceived of the study. YT and AI assisted experiments and statistical analysis. IM and TS participated in its full design and coordination, and DG, SI and AK participated in discussions.

Acknowledgements

This work was supported in part by a grant from The Japanese Ministry of Science and Culture (IM, TS).

References

1. Schubert D, Maier B, Morawietz L, Krenn V, Kamradt T: **Immunization with glucose-6-phosphate isomerase induces T cell-dependent peripheral polyarthritis in generally unaltered mice.** *J Immunol* 2004, **172:**4503-4509.
2. Iwanami K, Matsumoto I, Tanaka-Watanabe Y, Mihira M, Ohsugi Y, Mamura M, Goto D, Ito S, Tsutsumi A, Kishimoto T, Sumida T: **Crucial role of IL-6/IL-17 axis in the induction of arthritis by glucose-6-phosphate isomerase.** *Arthritis Rheum* 2008, **58:**754-763.
3. Matsumoto I, Zhang H, Yasukochi T, Iwanami K, Tanaka Y, Inoue A, Goto D, Ito S, Tsutsumi A, Sumida T: **Therapeutic effects of antibodies to tumor necrosis factor-α, interleukin-6 and cytotoxic T-lymphocyte antigen 4 immunoglobulin in mice with glucose-6-phosphate isomerase induced arthritis.** *Arthritis Res Ther* 2008, **10:**R66.
4. Brand DD, Myers LK, Terato K, Whittington KB, Stuart JM, Kang AH, Rosloniec EF: **Characterization of the T cell determinants in the induction of autoimmune arthritis by bovine α1(II)-CB11 in H-2^q mice.** *J Immunol* 1994, **152:**3088-3097.
5. Matsumoto I, Lee DM, Goldbach-Mansky R, Sumida T, Hitchon CA, Schur PH, Anderson RJ, Coblyn JS, Weinblatt ME, Brenner M, Duclos B, Pasquali JL, El-Gabalawy H, Mathis D, Benoist C: **Low prevalence of antibodies to glucose-6-phosphate isomerase in patients with rheumatoid arthritis and a spectrum of other chronic autoimmune disorders.** *Arthritis Rheum* 2003, **48:**944-954.
6. Matsumoto I, Staub A, Benoist C, Mathis D: **Arthritis provoked by linked T and B recognition of a glycolytic enzyme.** *Science* 1999, **286:**1732-1735.
7. **MHCPred** [http://www.jenner.ac.uk/MHCPred/]
8. Kawamoto T: **Use of a new adhesive film for the preparation of multi-purpose fresh-frozen sections from hard tissues, whole-animals, insects and plants.** *Arch Histol Cytol* 2003, **66:**123-143.
9. Bayrak Ş, Holmdahl R, Travers P, Lauster R, Hesse M, Dölling R, Mitchison NA: **T cell response of I-A^q mice to self type II collagen: meshing of the binding motif of the I-A^q molecule with repetitive sequences results in autoreactivity to multiple epitopes.** *Int Immunol* 1997, **9:**1687-1699.
10. Chen JS, Lorenz RG, Goldberg J, Allen PM: **Identification and characterization of a T cell-inducing epitope of bovine ribonuclease that can be restricted by multiple class II molecules.** *J Immunol* 1991, **147:**3672-3678.
11. Fritz RB, Skeen MJ, Chou CH, Garcia M, Egorov IK: **Major histocompatibility complex-linked control of the murine immune response to myelin basic protein.** *J Immunol* 1985, **134:**2328-2332.
12. Sakai K, Sinha AA, Mitchell DJ, Zamvil SS, Rothbard JB, McDevitt HO, Steinmann L: **Involvement of distinct murine T-cell receptors in the autoimmune encephalitogenic response to nested epitopes of myelin basic protein.** *Proc Natl Acad Sci USA* 1988, **85:**8608-8612.
13. Myers LK, Cooper SW, Terato K, Seyer JM, Stuart JM, Kang AH: **Identification and characterization of a tolerogenic T cell determinant within residues 181–209 of chick type II collagen.** *Clin Immunol Immunopathol* 1995, **75:**33-38.
14. Michaëlsson E, Andersson M, Engström A, Holmdahl R: **Identification of an immunodominant type-II collagen peptide recognized by T cells in H-2^q mice: self tolerance at the level of determinant selection.** *Eur J Immunol* 1992, **22:**1819-1825.
15. Myers LK, Seyer JM, Stuart JM, Terato K, David CS, Kang AH: **T cell epitopes of type II collagen that regulate murine collagen-induced arthritis.** *J Immunol* 1993, **151:**500-505.
16. Basu D, Horvath S, Matsumoto I, Fremont DH, Allen PM: **Molecular basis for recognition of an arthritic peptide and a foreign epitope on distinct MHC molecules by a single TCR.** *J Immunol* 2000, **164:**5788-5796.
17. Bettelli E, Carrier Y, Gao W, Korn T, Strom TB, Oukka M, Weiner HL, Kuchroo VK: **Reciprocal developmental pathways for the generation of pathogenic effector T_H17 and regulatory T cells.** *Nature* 2006, **441:**235-238.
18. Mangan PR, Harrington LE, O'Quinn DB, Helms WS, Bullard DC, Elson CO, Hatton RD, Wahl SM, Schoeb TR, Weaver CT: **Transforming growth factor-beta induces development of the T (H) 17 lineage.** *Nature* 2006, **441:**231-234.
19. He D, Wu L, Kim HK, Li H, Elmets CA, Xu H: **CD8+ IL-17 producing T cells are important effector functions for the elicitation of contact hypersensitivities responses.** *J Immunol* 2006, **177:**6852-6858.

20. Michel ML, Keller AC, Paget C, Fujio M, Trottein F, Savage PB, Wong CH, Schneider E, Dy M, Leite-de-Moraes MC: **Identification of an IL-17-producing NK1.1neg iNKT cell population involved in airway neutrophilia.** *J Exp Med* 2007, **204:**995-1001.
21. Yoshiga Y, Goto D, Segawa S, Ohnishi Y, Matsumoto I, Ito S, Tsutsumi A, Taniguchi M, Sumida T: **Invariant NKT cells produce IL-17 through IL-23-dependent and -independent pathways with potential modulation of Th17 response in collagen-induced arthritis.** *Int J Mol Med* 2008, **22:**369-374.
22. Lockhart E, Green AM, Flynn JL: **IL-17 production is dominated by gammadelta T cells rather than CD4 T cells during Mycobacterium tuberculosis infection.** *J Immunol* 2006, **177:**4662-4669.
23. Matsumoto I, Maccioni M, Lee DM, Maurice M, Simmons B, Brenner M, Mathis D, Benoist C: **How antibodies to a ubiquitous cytoplasmic enzyme may provoke joint-specific autoimmune disease.** *Nat Immunol* 2002, **3:**360-365.
24. Ranges GE, Sriram S, Cooper SM: **Prevention of type II collagen-induced arthritis by in vivo treatment with anti-L3T4.** *J Exp Med* 1985, **162:**1105-1110.
25. Williams RO, Whyte A: **Anti-CD4 monoclonal antibodies suppress murine collagen-induced arthritis only at the time of primary immunization.** *Cell Immunol* 1996, **170:**291-295.
26. Terato K, Harper DS, Griffiths MM, Hasty DL, Ye XJ, Cremer MA, Seyer JM: **Collagen-induced arthritis in mice: synergistic effect of E. coli lipopolysaccharide bypasses epitope specificity in the induction of arthritis with monoclonal antibodies to type II collagen.** *Autoimmunity* 1995, **22:**137-147.
27. Constant S, Pfeiffer C, Woodard A, Pasqualini T, Bottomly K: **Extent of T cell receptor ligation can determine the functional differentiation of naïve CD4+ T cells.** *J Exp Med* 1995, **182:**1591-1596.
28. Leitenberg D, Boutin Y, Constant S, Bottomly K: **CD4 regulation of TCR signaling and T cell differentiation following stimulation with peptides of different affinities for the TCR.** *J Immunol* 1998, **161:**1194-1203.
29. Bockermann R, Schubert D, Kamradt T, Holmdahl R: **Induction of a B-cell-dependent chronic arthritis with glucose-6-phosphate isomerase.** *Arthritis Res Ther* 2005, **7:**R1316-R1324.
30. Critchfield JM, Racke MK, Zúòiga-Pflücker JC, Cannellla B, Raine CS, Goverman J, Lenardo MJ: **T cell deletion in high antigen dose therapy of autoimmune encephalomyelitis.** *Science* 1994, **263:**1139-1143.
31. Gaur A, Wiers B, Liu A, Rothbard J, Fathman CG: **Amelioration of autoimmune encephalomyelitis by myelin basic protein synthetic peptide-induced anergy.** *Science* 1992, **258:**1491-1494.
32. Kori Y, Matsumoto I, Zhang H, Yasukochi T, Hayashi T, Iwanami K, Goto D, Ito S, Tsutsumi A, Sumida T: **Characterisation of Th1/Th2 type, glucose-6-phosphate isomerase reactive T cells in the generation of rheumatoid arthritis.** *Ann Rheum Dis* 2006, **65:**968-969.

Comprehensive Gene Expression Profiling of Peyer's Patch M Cells, Villous M-Like Cells, and Intestinal Epithelial Cells[1]

Kazutaka Terahara,[2*‡] Masato Yoshida,[2*†] Osamu Igarashi,[*‡] Tomonori Nochi,[*‡] Gemilson Soares Pontes,[*] Koji Hase,[§] Hiroshi Ohno,[§] Shiho Kurokawa,[*] Mio Mejima,[*] Naoko Takayama,[*†] Yoshikazu Yuki,[*‡] Anson W. Lowe,[¶] and Hiroshi Kiyono[3*†‡]

Separate populations of M cells have been detected in the follicle-associated epithelium of Peyer's patches (PPs) and the villous epithelium of the small intestine, but the traits shared by or distinguishing the two populations have not been characterized. Our separate study has demonstrated that a potent mucosal modulator cholera toxin (CT) can induce lectin *Ulex europaeus* agglutinin-1 and our newly developed M cell-specific mAb NKM 16-2-4-positive M-like cells in the duodenal villous epithelium. In this study, we determined the gene expression of PP M cells, CT-induced villous M-like cells, and intestinal epithelial cells isolated by a novel approach using FACS. Additional mRNA and protein analyses confirmed the specific expression of glycoprotein 2 and myristoylated alanine-rich C kinase substrate (MARCKS)-like protein by PP M cells but not CT-induced villous M-like cells. Comprehensive gene profiling also suggested that CT-induced villous M-like cells share traits of both PP M cells and intestinal epithelial cells, a finding that is supported by their unique expression of specific chemokines. The genome-wide assessment of gene expression facilitates discovery of M cell-specific molecules and enhances the molecular understanding of M cell immunobiology. *The Journal of Immunology*, 2008, 180: 7840–7846.

As a unique epithelial cell type specializing in Ag sampling, microfold or membranous cells (M cells) are present in the follicle-associated epithelium (FAE)[4] of both GALT and nasopharynx-associated lymphoid tissue, which act as a major inductive site for Ag-specific mucosal immune responses (1, 2). Recently, we also identified M cells in the small intestinal villous epithelium, at effector sites far from the FAE, suggesting that Ag sampling via villous M cells may be responsible for induction of systemic Ag-specific immune responses, such as IgG production via the oral route (3). Still missing, however, were a characterization of the shared and distinctive traits of Peyer's patches (PPs) and villous M cells and a better understanding of the immunological nature of each.

*Division of Mucosal Immunology, Department of Microbiology and Immunology, The Institute of Medical Science and †Department of Medical Genome Science, Graduate School of Frontier Science, The University of Tokyo, Tokyo, ‡Core Research for Evolutional Science and Technology, Japan Science and Technology Corporation, Saitama, and §Laboratory of Epithelial Immunobiology, Research Center for Allergy and Immunology, Institute of Physical and Chemical Research, Yokohama, Japan; and ¶Department of Medicine, Stanford University, Stanford, CA 94305

Received for publication February 12, 2007. Accepted for publication April 3, 2008.

The costs of publication of this article were defrayed in part by the payment of page charges. This article must therefore be hereby marked *advertisement* in accordance with 18 U.S.C. Section 1734 solely to indicate this fact.

[1] This work was supported in part by grants from Core Research for Evolutional Science and Technology of the Japan Science and Technology Corporation, the Ministry of Education, Science, Sports, and Culture, and the Ministry of Health and Welfare in Japan.

[2] K.T. and M.Y. contributed equally to this work and share first authorship.

[3] Address correspondence and reprint requests to Dr. Hiroshi Kiyono, Division of Mucosal Immunology, Department of Microbiology and Immunology, The Institute of Medical Science, The University of Tokyo, 4-6-1 Shirokanedai, Minato-ku, Tokyo 108-8639, Japan. E-mail address: kiyono@ims.u-tokyo.ac.jp

[4] Abbreviations used in this paper: FAE, follicle-associated epithelium; 7-AAD, 7-amino actinomycin; CKLF, chemokine-like factor; CT, cholera toxin; DAPI, 4′-6-diamidino-2-phenylindole; IEC, intestinal epithelial cell; IEL, intraepithelial lymphocyte; ISH, in situ hybridization; MLP, myristoylated alanine-rich C kinase substrate (MARCKS)-like protein; PP, Peyer's patch; UEA-1, *Ulex europaeus* agglutinin-1; WGA, wheat germ agglutinin.

Recent comprehensive gene expression analyses using microdissected FAE or whole cells dissociated from the FAE identified genes specifically expressed by PP M cells (4–6). Similar data, however, have not been available for villous M cells, in part because sufficient numbers of M cells are difficult to isolate from the surrounding intestinal epithelial cells (IECs). In mice, lectin *Ulex europaeus* agglutinin-1 (UEA-1) possessing affinity for α (1, 2) fucose has been routinely used for the detection of such M cells (3, 7). UEA-1, however, does not alone suffice to identify M cells because it also reacts to goblet cells (3). Our laboratory has recently succeeded in distinguishing M cells from goblet cells by developing a mAb (NKM 16-2-4 mAb) that specifically reacts to murine PP and villous M cells but not goblet cells and IECs (8). Furthermore, our recent separate studies have demonstrated that oral administration of cholera toxin (CT) as mucosal adjuvant resulted in the induction of NKM 16-2-4 mAb$^+$ and UEA-1$^+$ M-like cells, which have pocket structure and Ag uptake ability, in the duodenal villous epithelium (Terahara et al., submitted for publication). These recent advances in our understanding of M cells allowed us to define gene expression profiles capable of distinguishing PP M cells, CT-induced villous M-like cells, and IECs.

Materials and Methods

Animals

BALB/c mice were purchased from Japan SLC. These mice were maintained under specific pathogen-free conditions in horizontal flow cabinets in our experimental animal facility at the University of Tokyo. Following a previously established protocol (9, 10), CT (List Biologic Laboratories) was dissolved in PBS (20 μg/mouse) and then orally administered to BALB/c mice. Two days after CT administration, mice were used for experiments. All animal experiments were approved by the Animal Care and Use Committee of University of Tokyo.

Lectins and Abs for the detection of M cells

The following fluorescence-conjugated lectins and Abs were used for the identification of PP and villous M cells by FACS and histochemistry: PE-conjugated UEA-1 (Biogenesis), rhodamine-conjugated UEA-1 (Vector

Laboratories), biotin-conjugated UEA-1 (Vector Laboratories), FITC-conjugated wheat germ agglutinin (WGA) (Vector Laboratories), FITC-conjugated or biotin-conjugated M cell-specific NKM 16-2-4 mAb (8), and allophycocyanin-Cy7-conjugated anti-mouse CD45 mAb (30-F11; BD Biosciences).

Isolation of PP M cells, CT-induced villous M-like cells, and IECs

PPs from the naive duodenum and PP-free segments from the duodenum of naive or CT-administered mice were washed with cold PBS. Cells were dissociated from the small intestinal epithelium using a previously described mechanical procedure with some modifications (11). In brief, the tissues were incubated in PBS containing 0.5 mM EDTA with a stirrer for 10 min at 37°C. More than 90% of the dissociated cells survived as confirmed by a trypan blue exclusion test. The cells were stained with 1 μg/ml FITC-conjugated NKM 16-2-4 mAb, 5 μg/ml PE-conjugated UEA-1, and 1 μg/ml allophycocyanin-Cy7-conjugated anti-mouse CD45 mAb for 40 min before being reacted with 7-amino actinomycin (7-AAD; BD Biosciences) diluted 1/5 in DMEM containing 10% FCS for 10 min on ice. After washing with DMEM containing 10% FCS, the stained cells were analyzed using a flow cytometer FACSAria (BD Biosciences), and suitable cell populations gated on $CD45^-$ and $7\text{-}AAD^-$ cells were sorted.

DNA microarray analysis

Total RNA was extracted from the freshly isolated PP M cells, CT-induced villous M-like cells, and IECs of BALB/c mice using a High Pure RNA Tissue kit (Roche). Biotinylated cRNA was prepared using a two-cycle target-labeling assay in accordance with the protocol of the manufacturer (Affymetrix). The cRNA was hybridized with DNA probes on a GeneChip Mouse Genome 430 2.0 array (Affymetrix), washed, and fluorescence-labeled in accordance with the standard amplification protocol for eukaryotic targets developed by Affymetrix. The arrays were scanned with a GeneChip Scanner 3000 7G (Affymetrix). The fluorescence intensity of each probe was taken to represent the raw expression level and was quantified using GeneChip Operating software (Affymetrix). Data obtained from three independent experiments for PP M cells, CT-induced villous M-like cells, and IECs were normalized and statistically analyzed by Welch's ANOVA using GeneSpring 7.3.1 software (Silicon Genetics). In addition, both qualitative indices ("Present Call," "Marginal Call," and "Absent Call") based on *p*-value and a quantitative index (raw value) were also determined using GeneSpring 7.3.1 software. All microarray data described in this study have been deposited in the National Center for Biotechnology Information Gene Expression Omnibus database (www.ncbi.nlm.nih.gov/geo/) with the accession no. GSE7838.

In situ hybridization (ISH)

DNA fragments encoding GP2 (GenBank: NM_025989) and myristoylated alanine-rich C kinase substrate (MARCKS)-like protein (MLP; GenBank: NM_010807) were amplified by PCR from PP FAE-derived cDNA. The following sets of primers were used: *GP2*, sense, 5′-GGGTGATGGAGG AGTGAAGA-3′, anti-sense, 5′-CTCCAGGATGTTCCCACAGT-3′; and *MLP*, sense, 5′-*AATTAACCCTCACTAAAGGG*GAAGGCCAACGGACAG GAGA-3′, anti-sense, 5′-*TAATACGACTCACTATAGGG*CTTCTTGGGG GTCTCCTTGG-3′ (T3 and T7 promoter sequences are shown by italics). The PCR products for GP2 were subcloned into a pCR4-TOPO vector (Invitrogen). After sequencing, digoxigenin-labeled sense and anti-sense RNA probes were transcribed in vitro from the subcloned plasmids or from T3 and T7 promoter-conjugated PCR products with DIG RNA labeling mix (Roche). Paraffin-embedded sections of small intestinal tissues (6 μm) from naive BALB/c mice were obtained from Genostaff. ISH was performed as previously described (12). The bound probes were detected with BM purple AP substrate (Roche), before being counterstained with Kernechtrot stain solution (Muto Pure Chemicals) or reacted with 0.25 μg/ml biotin-conjugated UEA-1 at 4°C overnight after treatment with 3% H_2O_2. The sections labeled with biotin-conjugated UEA-1 were further reacted with HRP-conjugated streptavidin, followed by staining with 3,3′ diaminobenzidine (Vector Laboratories).

Generation of GP2- and MLP-specific Abs

For the generation of GP2- and MLP-specific Abs, the open reading frames of *GP2* and *MLP* genes were amplified by PCR from PP FAE-derived cDNA. The following sets of primers were used: *GP2*, sense, 5′-GACA T*GCTAGC*ATGAAAAGGATGGTGGGTTGTGAC-3′, anti-sense, 5′-GT ATC*GAATTC*TCAGAACAGTAGAGCCAGGAAGAC-3′; and *MLP*, sense, 5′-TGACT*GAATTC*ATGGGCAGCCAGAGCTCTAAGGCT-3′, anti-sense, 5′-TACAT*GTCGAC*CTACTCATTCTGCTCAGCACTGGC-3′,

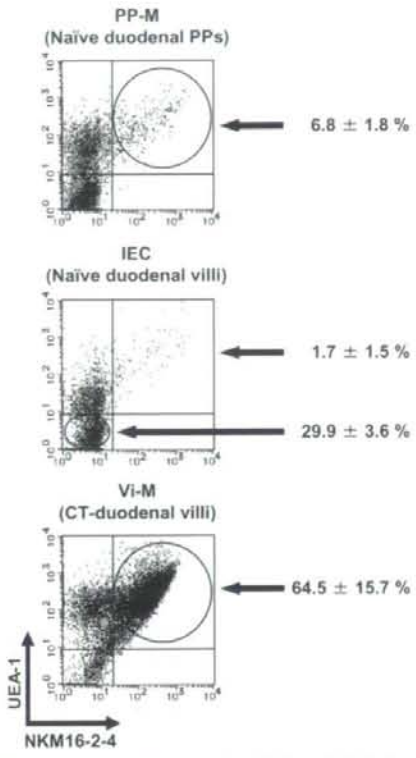

FIGURE 1. Frequency of PP M cells (PP-M) and CT-induced villous M-like cells (Vi-M) in the duodenal epithelium. Dot plots are shown by NKM 16-2-4-FITC and UEA-1-PE staining gated on $CD45^-$ and $7\text{-}AAD^-$ duodenal epithelial cell populations from naive BALB/c mice or from those that had been orally treated with CT. PP-M (NKM 16-2-4$^+$ and UEA-1$^+$), Vi-M (NKM 16-2-4$^+$ and UEA-1$^+$), and IEC (NKM 16-2-4$^-$ and UEA-1$^-$) were isolated by FACS. Numbers are the mean percentage ± SD in $CD45^-$ and $7\text{-}AAD^-$ epithelial cell populations from three independent experiments.

[*Nhe*I and *Eco*RI (*GP2*), and *Eco*RI and *Sal*I (*MLP*) restriction enzyme sites are shown by italics]. For generation of GP2-specific mAbs, amplified *GP2* gene was subcloned into pIRES2-EGFP vector (BD Biosciences) and the plasmid (pIRES2-GP2-EGFP) was then introduced in rat IEC line IEC-6 (ATCC, CRL-1592). After 2 days of transformation, EGFP-positive cells were purified by FACSAria and injected into the footpads of SD rats (1×10^6 cells/rat) five times at 2-wk intervals with TiterMax Gold (TiterMax) as an adjuvant. Four days after the final immunization, lymphocytes isolated from inguinal lymph node of the immunized rats were fused with P3×63-AG8.653 myeloma cells (ATCC, CRL-1580) in the presence of 50% (w/v) polyethylene glycol 1500 (Roche). Established hybridomas were injected into Crlj; CD1-*Foxn1*^{nu} mice and mAbs were purified from ascites by using Protein G-Sepharose (GE Healthcare). For generation of MLP-specific polyclonal Abs, the amplified *MLP* gene was subcloned into pGEX-4T-1 (GE Healthcare) and the plasmid (pMLP-GEX-4T-1) was then introduced in *Escherichia coli* DH5α. After induction of MLP expression with 0.1 mM isopropyl β-D-thiogalactoside, the GST-fused MLP was purified on a Glutathione-Sepharose 4B (GE Healthcare) and subsequently removed the GST-tag with thrombin (GE Healthcare). The purified rMLP was then immunized into New Zealand white rabbits and anti-MLP pAbs were purified from the antiserum by using rMLP-conjugated TOYOPEARL AF-Tresyl-650M (Tosoh).

Histochemical analysis

The histochemical analyses were performed with whole-mount tissues and frozen-section specimens prepared from mucus-free tissues fixed with 4% paraformaldehyde in PBS as previously described (3). For GP2 staining,

A

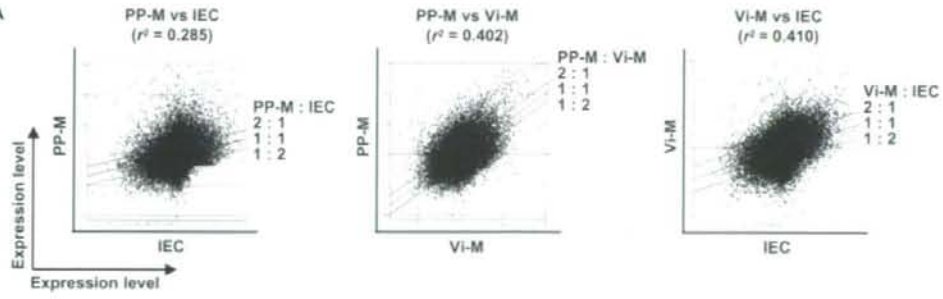

B

Group	Description	Criterion
A	PP-M-significant	1. "Present" or "Marginal Call" together with ≥ 100 raw value is shown in a cell fraction but not in the other two cell fractions.
B	Vi-M-significant	2. A normalized expression signal in a cell fraction is two-fold or higher than that seen in the other two cell fractions.
C	IEC-significant	
D	Sharing between PP-M and Vi-M	1. "Present" or "Marginal Call" together with ≥ 100 raw value is shown in two cell fractions but not in another cell fraction.
E	Sharing between PP-M and IEC	2. Each normalized expression signal in two cell fractions is two-fold or higher than that in another cell fraction.
F	Sharing between Vi-M and IEC	
G	Sharing in all cell fractions	1. "Present" or "Marginal Call" together with ≥ 100 raw value is shown in all cell fractions.

C

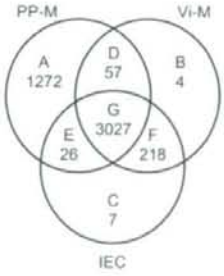

FIGURE 2. Gene expression profiles for PP M cells (PP-M), CT-induced villous M-like cells (Vi-M), and IECs. *A*, Scatter plots of the normalized expression level on each DNA microarray probe for PP-M and IEC, PP-M and Vi-M, and Vi-M and IEC with correlation coefficients (r^2). *B*, Grouping of probes based on their significance for PP-M, Vi-M, and IEC using the criteria outlined in the qualitative ("Present Call" or "Marginal Call") and quantitative (raw value) indices as assessed by GeneSpring 7.3.1 software. *C*, Venn diagram showing the categorization of significant probes into seven groups (Group A–G).

the specimens were incubated with 1 μg/ml rat anti-GP2 mAb (10F5-9-2) or the isotype control Ab (rat IgG2a; BD Biosciences) at 4°C overnight. For MLP staining, tissue sections were incubated with 10 μg/ml anti-MLP pAb or normal rabbit IgG at 4°C overnight. The specimens were then treated with 3 μg/ml Cy5-conjugated donkey anti-rat IgG or 3 μg/ml Cy5-conjugated donkey anti-rabbit IgG (Jackson ImmunoResearch Laboratories) together with 10 μg/ml tetramethylrhodamine isothiocyanate-conjugated UEA-1 (Vector Laboratories) and/or 5 μg/ml FITC-conjugated WGA (Vector Laboratories) for 1 h at room temperature. Finally, the section specimens were reacted with 400 ng/ml 4′-6-diamidino-2-phenylindole (DAPI; Sigma-Aldrich) and the signal was observed under a confocal laser-scanning microscope (TCS SP2; Leica). For counterstaining with our recently established M cell-specific mAb (NKM 16-2-4; rat IgG2c), the same section specimens were incubated with 5 μg/ml biotin-conjugated NKM 16-2-4 at 4°C overnight followed by 1.25 μg/ml HRP-conjugated streptavidin (Pierce) for 1 h at room temperature. The signal was then developed with 3,3′ diaminobenzidine and the nucleus was finally stained with hematoxylin.

Results

Isolation of PP M cells, CT-induced villous M-like cells, and IECs by FACS

FACS analysis demonstrated that the large forward-scatter CD45$^-$ cell population could be divided into three subpopulations by NKM 16-2-4 mAb and UEA-1 staining (Fig. 1). Because of the known specificities of NKM 16-2-4 mAb and UEA-1, cells positive for NKM 16-2-4 and UEA-1 were identified as M cells (or M-like cells) in this study. In the CD45$^-$ epithelial cell population isolated from the duodenum of naive BALB/c mice, the frequency of PP M cells averaged 7%. Perhaps due to the nature of the isolation technique used, the harvest of PP M cells far outstripped that of villous M cells, the frequency of the latter being so low (1.7 ± 1.5%) as to render harvest extremely difficult. We recently found that the number of villous M-like cells could be increased by oral administration of CT (64.5 ± 15.7% and Terahara et al., submitted for publication), and so decided to use the villous M-like cells induced by CT treatment for this DNA microarray analysis. A FACS with a purity of 90–99% was used to isolate PP M cells (NKM 16-2-4$^+$/UEA-1$^+$), CT-induced villous M-like cells (NKM 16-2-4$^+$/UEA-1$^+$), and IECs (NKM 16-2-4$^-$/UEA-1$^-$).

Assessment of gene expression profiling of PP M cells, CT-induced villous M-like cells, and IECs

DNA microarrays containing 45,101 probes were used to determine the comprehensive gene expression of PP M cells, CT-induced villous M-like cells, and IECs. Comparison of these

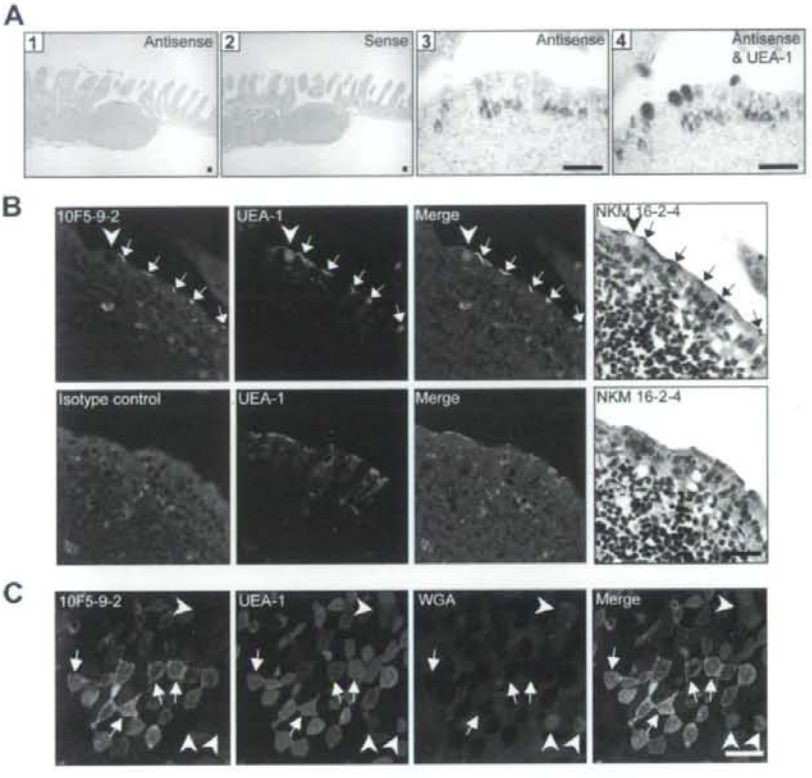

FIGURE 3. GP2 was specifically expressed by PP M cells in the small intestine. *A*, ISH for GP2 mRNA with positive signals (blue) of hybridized anti-sense or sense cRNA probes on duodenal PPs and adjacent villi of naive BALB/c mice. Tissues were also counterstained with Kernechtrot (pink, *1* and *2*) or labeled with UEA-1-HRP before being stained with 3,3′ diaminobenzidine (brown, *4*). *3* and *4*, High magnification of a PP FAE before (*3*) and after (*4*) labeling with UEA-1. Scale bar = 200 μm (*1* and *2*) and 40 μm (*3* and *4*). *B*, Confocal images of frozen sections of PPs stained with anti-GP2-specific mAb (10F5-9-2) or isotype control (rat IgG2a). The specific expression of GP2 in M cells was confirmed by counterstaining with our recently established M cell-specific mAb (NKM 16-2-4). Arrows and arrowheads show M cells and goblet cells, respectively. Scale bar = 30 μm. *C*, Confocal images of whole-mount duodenal PP domes stained with anti-GP2-specific mAb (10F5-9-2), UEA-1, and WGA. Scale bar = 30 μm.

profiles revealed correlation coefficients of 0.285 for PP M cells and IECs, of 0.402 for PP M cells and CT-induced villous M-like cells, and of 0.410 for CT-induced villous M-like cells and IECs (Fig. 2*A*). Based on the constructed gene profiling, we categorized probes showing significant expression into seven groups (Groups A-G) using our own criteria (Fig. 2*B*). The 1272, 4, and 7 probes were regarded as significant for PP M cells (Group A), CT-induced villous M-like cells (Group B), and IECs (Group C), respectively (Fig. 2*C*). The relative expression levels and gene names of the significant probes are provided in Supplementary Table I.[5] Our gene-profiling database allowed us to confirm previous findings that Group A includes the transcripts of peptidoglycan recognition protein-S, secretory granule neuroendocrine protein 1, and annexin V that are specifically expressed by PP M cells (4–6).

Specific expression of GP2 by PP M cells

In an effort to identify molecules that could be expressed on the apical surface of PP M cells, we looked for genes showing a higher expression level in Group A. During the ISH analysis, we found that GP2 mRNA was specifically expressed in the FAE of PPs throughout the small intestine (Fig. 3*A*, *1*) and that its expression was distinctively colocalized with UEA-1$^+$ M cells (Fig. 3*A*, *3* and *4*). A negative control using sense cRNA probes did not show any positive signals (Fig. 3*A*, *2*). Immunohistochemical analysis with newly established anti-GP2-specific mAb (10F5-9-2) revealed that the GP2 protein was highly expressed in UEA-1$^+$ PP M cells (Fig. 3*B*). A negative control using isotype rat IgG2a did not show any positive signals in the dome epithelium of PPs (Fig. 3*B*). The expression of GP2 in M cells was further confirmed by counterstaining with our recently established M cell-specific mAb NKM 16-2-4 (Fig. 3*B*). Supporting the histochemical analyses, whole-mount staining analysis also demonstrated GP2 was expressed on the apical surface of UEA-1$^+$ PP M cells, which were not recognized by enterocyte-reactive lectin WGA (Fig. 3*C*). Supporting the gene profiling data (Supplementary Table I), GP2 protein was not detected in CT-induced villous M-like cells (data not shown).

Unique expression of MLP by PP M cells in the small intestine

Candidates for FAE-specific genes including *MLP* (also known as *MacMARCKS* or *MRP*) have been previously proposed (5, 6). Most of these genes together with *MLP* could be identified as PP M cell-significant genes by the DNA microarray analysis (Supplementary Table I). The subsequent ISH analysis demonstrated a unique expression pattern of MLP mRNA in the small intestine, i.e., MLP mRNA was detected in the FAE and B cell zones of PPs throughout the small intestine (Fig. 4*A*, 1). A negative control using sense cRNA probes did not show any positive signals (Fig. 4*A*, 2). In the FAE, the expression of MLP mRNA was exclusively colocalized with UEA-1$^+$ M cells (Fig. 4*A*, 3 and 4). Immunohistochemical analysis further elucidated the complicated expression pattern of MLP, revealing that the MLP protein was also found in B cell zones and the cytoplasm of M cells in PPs throughout the small intestine (Fig. 4*B*), but not in CT-induced villous M-like cells (data not shown). A negative control using normal rabbit IgG did not show any positive signals (Fig. 4*B*).

[5] The online version of this article contains supplemental material.

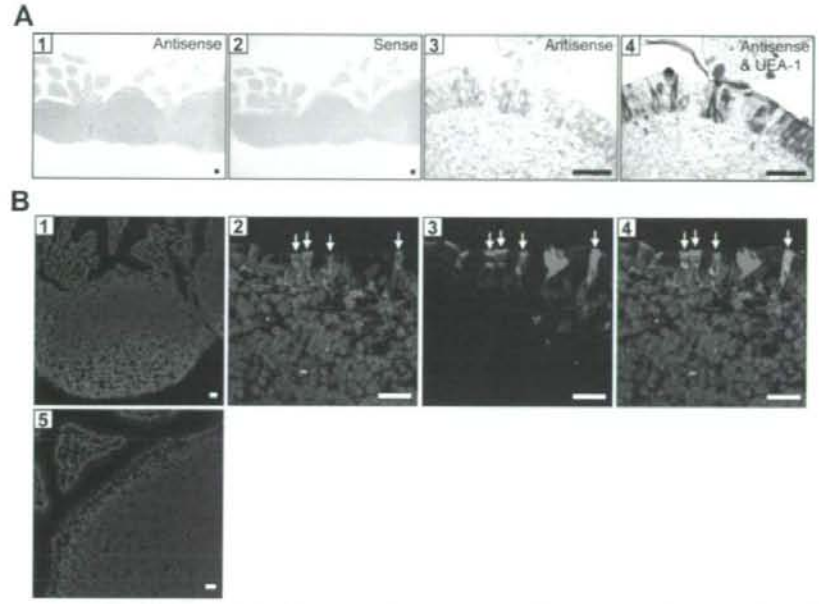

FIGURE 4. MLP was expressed by M cells and by the B cell zones of PPs but not by villi. *A*, ISH for MLP mRNA with positive signals (blue) of hybridized anti-sense or sense cRNA probes on duodenal PPs and adjacent villi of naive BALB/c mice. Tissues were also counterstained with Kernechtrot (pink, *1* and *2*) or labeled with UEA-1-HRP before being stained with 3,3′ diaminobenzidine (brown, *4*). *3* and *4*, High magnification of a PP FAE before (*3*) and after (*4*) labeling with UEA-1. Scale bar = 200 μm (*1* and *2*) and 40 μm (*3* and *4*). *B*, Confocal images of frozen sections of duodenal PPs stained with anti-MLP-specific pAb or control rabbit IgG. Confocal images of frozen sections of duodenal PPs from naive BALB/c mice labeled with UEA-1-rhodamine, DAPI, and immune complexes of FITC-labeled anti-rabbit IgG secondary Ab with anti-MLP polyclonal Ab or normal rabbit IgG. *1* and *5*, Merged images of DAPI (blue) and MLP (green) (*1*) or normal rabbit IgG (green) (*5*). *2–4*, High magnification of a PP FAE. *2*, Merged image of DAPI-(blue) and MLP (green)-staining. *3*, Single image of UEA-1-staining (red). *4*, Merged image of (*2*) and (*3*). Arrows show PP M cells expressing MLP. Scale bar = 100 μm (*1*), 50 μm (*5*), and 10 μm (*2–4*).

Unique expression of chemokines in PP M cells and/or CT-induced villous M-like cells

Focusing on chemokines whose presence was statistically identified regardless of the raw value, we found seven chemokines to be expressed by PP M cells and/or CT-induced villous M-like cells (Table I). In addition to the previously reported CCL9 and CCL20 that are expressed by the M cell-containing PP FAE (13–15), we found significant expression of CXCL13 and chemokine-like factor (CKLF) in PP M cells. Although CT-induced villous M-like cells and IECs constitutively expressed CCL6 and CCL28, the expression level of these chemokines was highest in PP M cells (thereby categorized in Group G; Fig. 2, *B* and *C*). Next, we also examined the expression pattern of chemokines in CT-induced villous M-like cells, finding, as in PP M cells, an up-regulation of CCL9, CKLF, and CCL6 mRNAs. Their raw values and expression levels were higher than those seen in IECs (Table I). Furthermore, CT-induced villous M-like cells showed the highest expression of CXCL16 mRNA, with expression levels 1.9–2.5-fold higher than in PP M cells and 2.1–2.3-fold higher than in IECs (Table I).

Table I. *Chemokines expressed by PP M cells and/or CT-induced villous M-like cells*[a]

Name	GenBank	Affymetrix Probe No.	Group (see Fig. 2C)	Relative Expression Level against IEC	
				PP-M	Vi-M
CCL9	AF128196	1417936_at	A	124.8	7.0
CXCL13	AF030636	1417851_at	A	64.4	-
CKLF	BE852312	1436242_a_at	A	52.2	8.3
CCL6	AV084904	1420249_s_at	G	30.4	5.1
	BC002073	1417266_at	G	12.5	4.6
CCL20	AF099052	1422029_at	A	10.9	-
CCL28	BE196980	1455577_at	G	2.8	0.7
CXCL16	BC019961	1449195_s_at	G	1.1	2.1
		1418718_at	G	0.9	2.3

[a] Expression levels on probes identified as "Present Call" in PP M cells (PP-M) or CT-induced villous M-like cells (Vi-M) were compared with those in IECs. Minus indicated no expression in Vi-M and IECs. CKLF, Chemokine-like factor.

Discussion

In this study, we combined the advanced techniques of M cell purification and DNA microarrays to construct a gene-profiling database for PP M cells, CT-induced villous M-like cells, and IECs. The lack of M cell-specific markers has long presented an obstacle to the isolation of M cells. We overcame this barrier by using M cell-specific NKM 16-2-4 mAb. Our knowledge that villous M (or M-like) cells, usually low frequency in the duodenum, could be increased by CT allowed us to separately isolate PP M cells, CT-induced villous M-like cells, and IECs using FACS. Of course, we cannot yet exclude the possibility that individual cell-sorted fractions were mildly contaminated by other cell types; however, we regard the database as reliable because most of the previously reported PP M cell-specific genes encoding peptidoglycan recognition protein-S, secretory granule neuroendocrine protein 1, and annexin V (4–6) were found in the PP M cell-significant group (Group A). Thus, the gene-profiling database presented

here has several advantages: it appears reliable because it was capable of confirming already established findings; it includes villous M (or M-like) cells as well as PP M cells and IECs; and it is based on a purified cell population. These advantages could make this gene-profiling database a reliable and useful tool for identifying new molecules expressed by M cells and for deepening our understanding of M cell immunobiology.

A mucosal vaccine delivery system targeting PP M cells would be more effective at generating not only efficient mucosal but also systemic immunity. When UEA-1 was used as an Ag delivery vehicle, the administration of PP M cell-targeted Ags induced Ag-specific mucosal and systemic immune responses (16) despite the cospecificity of the lectin for M cells and goblet cells (3). The gene-profiling database was, therefore, used to look for candidate target molecules in the vaccine delivery system. We focused on GP2, which is a GPI-anchored protein expressed at a higher level in Group A. GP2 is associated with lipid rafts, is sorted to the apical plasma membrane (17), and is likely to possess a similar distribution in PP M cells. Additional mRNA and protein analyses by ISH and immunohistochemistry identified the specific expression of GP2 in the apical plasma membrane of PP M cells. Although the role played by GP2 in a unique Ag-sampling system of PP M cells remains obscure, GP2 is not required for PP M cell development, as evidenced by the presence of M cells in the FAE of PPs from *GP2*$^{-/-}$ mice (data not shown). Taken together, these findings support the candidacy of GP2 as an M cell-targeting molecule. If it is in fact confirmed to be so, it could greatly contribute to the development of a mucosal vaccine delivery system.

In addition to the identification of GP2, reliance of the gene-profiling database is further supported by the identification of specific expression of MLP by PP M cells. Not only *MLP* but also other genes have been previously reported as FAE-specific genes (5, 6). Using DNA microarray analysis, we were able to identify most such genes, including *MLP*, as PP M cell-significant genes. This study demonstrated for the first time the histological distribution of expressed MLP mRNA and protein in the small intestine. MLP, a member of protein kinase C substrates, binds calcium/calmodulin and actin (18, 19), and has been implicated in integrin-dependent phagocytosis by macrophages (20, 21). However, that contention was challenged in another study by Underhill and coworkers (22) using *MLP*$^{-/-}$ macrophages. Interestingly, β1 integrin, which is expressed by the apical membrane of PP M cells but not of IECs in the murine small intestine, is involved in the uptake of *Yersinia* by PP M cells via integrin-invasin binding (23). Thus, MLP may also account for the Ag uptake/sampling process, including integrin-dependent Ag uptake, of M cells located within the FAE of PPs.

Our constructed gene profiling also provides additional information for M cell immunobiology. Both PP and villous M cells contain in their basolateral region immunocompetent cells characterized by a pocket formation (3, 24), the contents of which are influenced by the repertoire of chemokines expressed by M cells. So far, three chemokines, CCL9, CCL20, and CXCL16, have been reported to be specifically expressed by the M cell-containing FAE of PPs and to contribute to the spatial distribution of dendritic cells or T cells in the subepithelial dome as well as in the basolateral pocket regions of M cells (13–15, 25). Our examination for the gene expression pattern of chemokines using the gene-profiling database showed that CXCL13, CKLF, CCL6, and CCL28, in addition to CCL9 and CCL20, are specifically or highly expressed by PP M cells, suggesting that CXCL13, CKLF, CCL6, and CCL28 may also play a role in regulating the recruitment of various immunocompetent cells into the pocket region of PP M cells.

Noticeably, CT-induced villous M-like cells share with PP M cells the expression of certain chemokines, including CCL6, CCL9, and CKLF. Furthermore, the highest expression of CXCL16 mRNA was observed in CT-induced villous M-like cells, although CXCL16 has previously been shown to be specifically expressed in the FAE of PPs (25). This discrepancy may result from our exclusive use of duodenal tissues for the analysis of M cell gene profiling. CXCL16 is a chemoattractant for activated CD8$^+$ T cells and, to a lesser extent, for activated CD4$^+$ T cells (25, 26); the CXCL16 receptor is expressed by intraepithelial lymphocytes (IELs) (26). In the small intestine, the distribution patterns for CD4$^+$ and CD8$^+$ T cells are distinct, with CD4$^+$ T cells primarily located in the lamina propria and CD8$^+$ T cells residing along the epithelium (27). When CT was orally administered, CD8$^+$ IELs were rapidly and transiently depleted (28). Interestingly, we observed that CD8$^+$ IEL numbers recovered following the generation of CT-induced villous M-like cells (data not shown). Therefore, our current finding that CT-induced villous M-like cells express a higher level of CXCL16 makes it plausible that CD8$^+$ T cells are retained in the intestinal epithelium, mainly into the pocket of villous M-like cells. Furthermore, up-regulation of CCL9, CKLF, CCL6, and CXCL16 in CT-induced villous M-like cells could account for the CT-induced recruitment of immunocompetent cells to the site of Ag sampling from the intestinal lumen via CT-induced villous M-like cells.

Although the development mechanism of villous M cells remains unclear, we hypothesize that villous M cells are differentiated from IECs by exogenous stimuli because oral CT administration resulted in the induction of villous M-like cells in the middle to upper regions of villi (Terahara et al., submitted for publication), i.e., where IECs normally migrate from the crypts to the villus (29). Our hypothesis is also informed by the suggestions offered by other groups that IECs in the FAE of PPs could be converted to M cells by bacterial infection and inflammation (30, 31). We propose that CT-induced villous M-like cells have a gene expression pattern that is intermediate between PP M cells and IECs, as evidenced by the very similar correlation coefficient values obtained when the comprehensive gene profile of CT-induced villous M-like cells was compared with that of PP M cells (r^2 = 0.402) and IECs (r^2 = 0.410). The intermediate nature of CT-induced villous M-like cells between PP M cells and IECs is further confirmed by chemokine expression profiles. In this study, we have attempted to use gene profiling to elucidate the development mechanism of villous M cells.

In conclusion, our gene-profiling database should prove a valuable tool in identifying suitable M cell-targeting molecules, thereby speeding the development of a mucosal vaccine delivery system as well as allowing for a better understanding of M cell immunobiology.

Acknowledgments

We thank the members of our laboratory for technical advice and helpful discussions. We also extend our thanks to Dr. K. McGhee for editorial help.

Disclosures

The authors have no financial conflict of interest.

References

1. Gebert, A., H. J. Rothkötter, and R. Pabst. 1996. M cells in Peyer's patches of the intestine. *Int. Rev. Cytol.* 167: 91–159.
2. Neutra, M. R., A. Frey, and J. P. Kraehenbuhl. 1996. Epithelial M cells: gateways for mucosal infection and immunization. *Cell* 86: 345–348.
3. Jang, M. H., M. N. Kweon, K. Iwatani, M. Yamamoto, K. Terahara, C. Sasakawa, T. Suzuki, T. Nochi, Y. Yokota, P. D. Rennert, et al. 2004. Intestinal villous M